Chlorophyll derivatives with anti-obesity activity

Ricardo Figueiredo
Master in Functional Biology and Biotechnology of Plants
Biology department
2023

Supervisor
Dr Ralph Urbatzka, group leader of B4H Biodiscovery for Health at CIIMAR
& invited auxiliary professor at FCUP

Co-supervisor
Dr Mariana Reis, senior researcher at the BBE Blue Biotechnology and Ecotoxicology group at CIIMAR

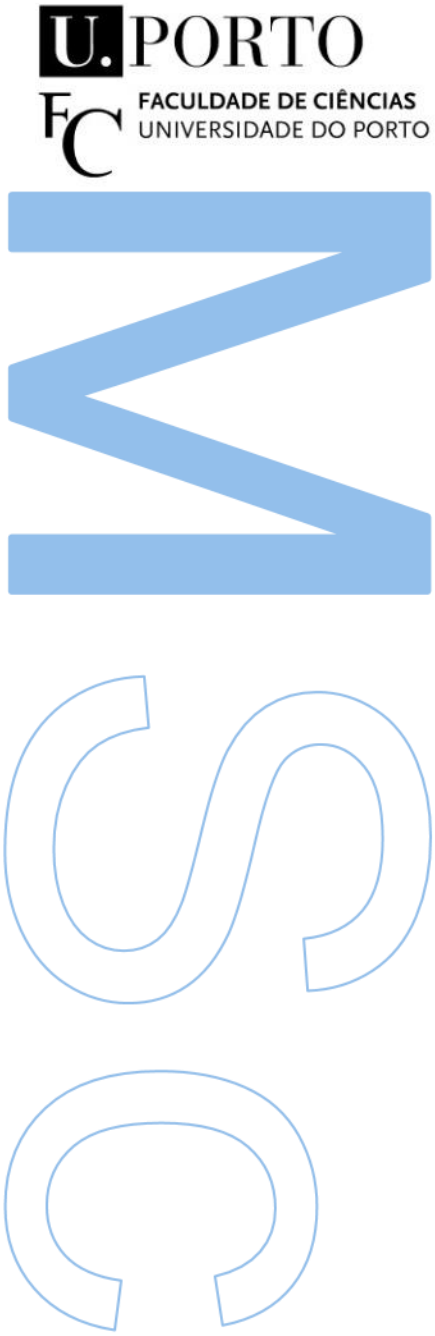


U.PORTO
FACULDADE DE CIÊNCIAS
UNIVERSIDADE DO PORTO

Acknowledgements

O processo de desenvolvimento e escrita desta tese não teria sido possível sem o apoio e acompanhamento de pessoas que me ajudaram e ensinaram ao longo do último ano. Assim, gostaria de começar por agradecer aos meus orientadores, o Doutor Ralph Urbatzka e a Doutora Mariana Reis, por toda a disponibilidade que sempre mostraram para responder às minhas dúvidas, bem como pela tranquilidade e ensinamentos que me foram transmitindo. Agradeço à Natália Silva por toda a paciência e ajuda fundamental ao desenvolvimento do trabalho prático e também à restante equipa do BBE pelo bom ambiente e pelos snacks que brotavam com uma regularidade que justifica parte da investigação que ali é feita.

Aos meus colegas e amigos Dora Ferreira, Lucas Solidade, Pedro Cruz, Rúben Luz, Leonor Ferreira, Catarina Fonseca e Filipe Henriques, pelos bons momentos dentro e fora do CIIMAR que, inadvertidamente, me foram abrindo a cabeça (metaforicamente, é claro).

Obrigado ao João e à Lécia, sem os quais o Porto não seria uma casa e por me ajudarem a levar as coisas mais na desportiva e a divertir-me pelo caminho. Obrigado pelos últimos dois anos.

Não poderia deixar de agradecer também aos meus amigos fora do Porto e do ambiente académico por me estimularem em outras áreas para além da ciência, seja através de conversas, convites inesperados ou sugestões que tanto me dão gosto ouvir. Um obrigado especial à Kiki, à Sofia, à Catarina, à Laura e ao Rui.

Por último, quero agradecer à minha família e, principalmente, aos meus pais e irmão por todo o apoio e orgulho que depositam em mim.

Este trabalho foi suportado pelo Pacto de Inovação (Projeto Nº. C644915664-00000026), designado por «Pacto da Bioeconomia Azul». O Pacto decorre da candidatura ao Aviso Nº 02/C05-i01/2022, no âmbito da Plano de Recuperação e Resiliência (PRR), integrando o investimento i01.01: Agendas/Alianças mobilizadoras para a Inovação Empresarial.

Resumo

A obesidade é uma doença complexa e multifatorial que assola uma parte crescente da população mundial. Está associada a diversas doenças cardiovasculares, psicológicas, etc. O tratamento desta doença multifatorial vai muito além de mudanças no estilo de vida. As atuais opções disponíveis acarretam alguns riscos para a saúde bem como inconveniências associadas às soluções mais invasivas. Assim, a investigação de novos tratamentos tem-se alargado à pesquisa das potencialidades de compostos naturalmente produzidos por organismos. Dentro destes produtos naturais, os derivados de clorofila têm despertado o interesse da comunidade científica dada a recente descoberta da capacidade de redução lipídica associada aos compostos: 13^2-hidroxifeofitina a e 13^2-hidroxifeofarnesina a.

Neste trabalho, procurou-se otimizar a extração de derivados de clorofila a partindo de biomassa de *Arthrospira platensis*, uma cianobactéria produtora de grandes quantidades deste pigmento, bem como de outros produtos naturais de interesse. Os extratos obtidos foram avaliados quanto às suas capacidades de redução lipídica e redução do apetite em larvas de peixe-zebra recorrendo ao bioensaio do metabolismo de gorduras com Nile Red e a um bioensaio baseado em lipossomas. Paralelamente, fez uma análise metabolómica *in silico*, recorrendo aos GNPS, bem como uma quantificação relativa de derivados de clorofila a selecionados utilizando a técnica de cromatografia líquida acoplada a espectrometria de massa. Deste modo foi possível estabelecer uma relação entre as condições de extração e as abundâncias relativas destes compostos, identificar os extratos bioativos e, por fim, identificar putativamente compostos presentes nos extratos bioativos.

Como resultado, 28 extratos foram obtidos, 9 dos quais mostraram ser capazes de promover uma redução lipídica e 4 extratos reduziram o apetite em larvas de peixe-zebra. Foi ainda possível identificar putativamente 9 compostos bem como produzir protocolos de extração para os diferentes derivados de clorofila a.

Palavras-chave: Derivados de Clorofila; *Arthrospira platensis*; Redução lipídica; Redução do apetite; GNPS.

Abstract

Obesity represents a complex and multifactorial disease that affects a growing segment of the global population. It is linked to a spectrum of cardiovascular and psychological diseases, among others. Addressing this multifactorial disease extends well beyond lifestyle changes. Current therapeutic options carry certain health risks and are accompanied by inconveniences, particularly in the context of more invasive interventions. Consequently, research of new treatments has expanded to explore the potential of compounds naturally produced by organisms. Within these natural products, chlorophyll derivatives have sparked the interest of the scientific community, owing to the recent discovery of their lipid-reducing activity, specifically the compounds 13^2-hydroxy-pheophytin a e 13^2-hydroxy-pheofarnesin a.

In this study, an optimisation of the extraction process of chlorophyll a and its derivatives was test from *Arthrospira platensis* biomass, a remarkable cyanobacterium that produces significant quantities of this pigment and other natural products of interest. The obtained extracts were evaluated for their lipid and appetite-reducing activities in zebrafish larvae performing the Nile Red fat metabolism bioassay and a liposome-based bioassay. Additionally, an *in silico* metabolomic analysis was conducted using the Global Natural Product Social Molecular Networking (GNPS) platform and relative quantification of selected chlorophyll a derivatives from liquid chromatography-mass spectrometry analyses. This approach allowed the establishment of a relationship between the extraction conditions and the relative abundances of the selected analysed compounds, the identification of bioactive extracts, and ultimately the putatively identification of compounds in these extracts.

As a result, 28 extracts were obtained, with 9 of them demonstrating the ability to promote lipid reduction and 4 extracts reducing appetite in zebrafish larvae. Additionally, 9 compounds were putatively identified in some bioactive extracts and extraction protocols were developed for different derivatives of chlorophyll a.

Keywords: Chlorophyll Derivatives; *Arthrospira platensis*; Lipid Reduction; Appetite Reduction; GNPS.

Table of Contents

List of Tables

List of Figures

List of Abbreviations

[M+H]$^+$ – Adducted mass

3'-CMP – Cyitidine 3'-monophosphate

5'-GMP – Guanosine-5'-monophosphate

AT – Adipose tissue

BAT – Brown adipose tissue

BMI – Body mass index

CEMUP – Materials Centre of the University of Porto

CFM-ID – Competitive fragmentation modelling for metabolite identification

CIIMAR – Interdisciplinary Centre of Marine and Environmental Research

DMSO – Dimethyl-sulfoxide

DPF – Days post fertilisation

EASO – European association for the study of obesity

ECM – Extracellular matrix

EFSA – European food safety authority

EtOH – Ethanol (CH_3CH_2OH)

EGT – Ergothioneine

FCUP – Faculdade de Ciências da Universidade do Porto

FDA – Food and drug administration

FLX – Fluoxetine hydrochloride

GLP-1 – Glucagon-like peptide-1

GNPS – Global natural products social molecular networking

GRAS – Generally regarded as safe

HPLC – High performance liquid chromatography

IL-6 – Interleukin-6

LC-HR ESI-MS/MS – Liquid chromatography - high resolution electrospray ionisation tandem mass spectrometry

LDL – Low-density lipoprotein

***m/z* –** Mass to charge ratio

MeOH – Methanol (CH_3OH)

MFI – Mean fluorescence intensity

MS^2 – Fragmentation spectra

MTA – 5'-methylthioadenosine

MS-222 – Tricaine

NAFLD – Non-alcoholic fatty liver disease

NAP – Network annotation propagation

NR – Nile Red

NPs – Natural products

ppm – Parts per million

PTU – 1-phenyl-2-thiourea

R^2 – Coefficient of determination

REV – Resveratrol

Rt – Retention time

SAM – S-adenosylmethionine

SVF – Stromal vascular fraction

T2DM – Type 2 diabetes mellitus

TNF-α - Tumor necrosis factor alpha

WAT – White adipose tissue

WHO – World health organisation

1. Introduction

1.1 Obesity: A Comprehensive Overview

Obesity is a serious and multifactorial disease characterised by excessive accumulation of fat. Despite this, fat distribution, whole-body inflammatory state, and genetics can also be used to diagnose this condition (1,2). Body mass index (BMI) is a statistical tool used to identify obesity in populations and it establishes a relationship between a person's weight and the square of their height in metres (kg/m^2). According to the World Health Organisation (WHO), an individual with a BMI over 30 kg/m^2 is classified as obese (3,4). However, this index exhibits low sensitivity, since body weight can increase due to muscle mass, for example. The substantial inter-individual variability in the percentual body fat for any given BMI value, partly attributed to factors such as age, sex, and ethnicity, also contributes to the low sensitivity of BMI. Hence, to diagnose obesity with more accuracy, several other factors should be considered beyond weight and height (5).

The causes of obesity extend far beyond an imbalanced diet and lack of physical activity. It results from a complex interplay of several factors, including genetic, psychological, social, economic, environmental, and even political influences (6,7). This epidemic is associated with various diseases that can lead to mortality, such as cardiovascular diseases, insulin resistance, type 2 diabetes mellitus (T2DM), metabolic syndrome, hyperlipidaemia, hypertension, non-alcoholic fatty liver disease (NAFLD), certain cancers (e.g., breast and ovarian), infertility, osteoporosis, sleep apnoea, and even depression (2,8,9).

Over the past few decades, obesity has emerged as a global concern, with its incidence rates increasing across the globe. The European Association for the Study of Obesity (EASO) underscores its gravity by attributing more deaths to obesity than underweight (10). In 2016, EASO stated that over 1.9 billion adults (≥ 18 years old) were overweight and 650 million of these were obese (10). This number has nearly tripled since 1975 (4,10). Childhood obesity is also a dramatic concern, in 2020, 39 million children (≤ 5 years old) were classified as obese or overweight (4). Portugal, like many other countries, is also grappling with this issue, as nearly 60% of the portuguese population was classified as obese or overweight by Oliveira *et al.*, in 2016 (11). However, in 2019, a longitudinal retrospective study from real-world data showed that the prevalence of obesity in the adult population (24 - 74 years) of northern Portugal was 10.2%, with a higher prevalence (16.1%) reported in the 65 – 74 age group (12).

Beyond its health implications, obesity represents a significant economic cost, with global costs equivalent to 2.19% of the global gross domestic product in 2019. This trend is expected to persist, with projections estimating costs to rise to 3.29% by 2060 (13). Responding to these stark realities, the WHO recommends reducing fat and sugar intake, increasing the consumption of vegetables, fruits, legumes, whole grains, and nuts, and engaging in, at least, 150 minutes of physical activity per week (4).

In summary, while lifestyle changes can be effective as a preventing tool, a comprehensive approach is craved for treatments. Exploring the intricate role of adipose tissue in the pathophysiology of obesity provides valuable insights. This understanding is crucial for developing and improving drug interventions, offering a promising path for better obesity management.

1.1.1 Adipose Tissue and Its Remodulation in Obesity

From yeast to humans, energy is stored in the form of lipid droplets, mainly triglycerides, in order to provide energy during periods when caloric demand exceeds caloric intake (14). Adipose tissue (AT) has evolved over thousands of years as an adaptive response to the need for energy storage. This connective tissue is a sophisticated and highly relevant metabolic and endocrine organ, regulating the whole-body metabolism and homeostasis, while also providing cohesion to the organs. It is mainly composed of adipocytes, an extracellular matrix (ECM), and a stromal vascular fraction (SVF) (15). Adipocytes account for most of the volume of AT, and their main function is the storage and release of fat. The ECM is composed of proteins such as collagen and elastin, as well as glycosaminoglycans, and provides structural support to AT. The SVF is a heterogeneous mixture of cells, including adipose-derived stem cells, endothelial cells, endothelial progenitor cells, pericytes, T cells, and other immune cells such as macrophages, lymphocytes, and eosinophils (15,16).

In mammals, this tissue can be categorised into two predominant types based on their functions, colouration, vascularisation, and structure: white adipose tissue (WAT) and brown adipose tissue (BAT). WAT, a highly adaptable tissue, is the most common in adult mammals. It appears white or yellow and is located subcutaneously, serving as the primary energy storage site in the body. Moreover, it secretes various hormones and factors, including adiponectin, resistin, leptin, and other cytokines. Conversely, BAT is responsible for thermogenesis. It is situated in both superficial and deep body sites, characterised by its brown hue due to the presence of mitochondria

and cytochromes. In addition to these types, a beige adipose tissue, also known as “brite”, can emerge from WAT through a transdifferentiation process known as “browning of WAT”, triggered by stimuli such as exercise, cold exposure, and other environmental factors. Alternatively, brite can originate through *de novo* differentiation from tissue-resident progenitors. This intermediate adipose tissue also actively contributes to thermogenesis, energy expenditure, and metabolic regulation processes (17–19).

In the context of obesity, AT undergoes significant changes that contribute to the overall pathology of this condition, such as metabolic dysfunction and cardiovascular complications. This remodelling of AT constitutes a key aspect of its pathophysiology. The excessive accumulation of fat, particularly in the visceral depots, triggers a cascade of changes that profoundly impact both metabolic and cardiovascular health. Notably, hypertrophic expansion of adipocytes is a hallmark of obesity-associated adipose tissue remodelling. As caloric intake surpasses expenditure, adipocytes increase their volume – hypertrophy – to accommodate excess lipids. However, hypertrophy is a limited process, leading to the recruitment and differentiation of adipocyte precursors to sustain lipid storage – hyperplasia. This dynamic hypertrophy-hyperplasia balance contributes to the plasticity of AT and its ability to cope with excess energy (15). Additionally, obesity-induced AT remodelling is accompanied by an alteration in immune cell composition, and the adipokines equilibrium is disrupted. Cytokines such as adipokines (e.g. adiponectin, leptin, and resistin) are linked to insulin regulation, and the reducing of their levels contributes to systemic insulin resistance. Conversely, the upregulation of pro-inflammatory cytokines, including interleukin-6 (IL-6) and tumour necrosis factor alpha (TNF-α), perpetuates a chronic low-grade inflammatory state within AT and the broader systemic environment (15,20).

Conclusively, delving into intricate repercussions of obesity on human physiology, particularly on AT remodelling, stands as an imperative pursuit. This investigation holds the key to advancing novel therapeutic interventions and refining existing strategies, thereby offering invaluable insights for the enhancement of medical approaches in this multifaceted domain.

1.2 Tackling Obesity: Current Approaches and Solutions

Obesity, as a complex and multifaceted metabolic disorder, often lacks a singular cause or cure. In response, innovative therapies are being developed alongside lifestyle changes recommended by the WHO (4). Presently, the landscape includes bariatric surgery and pharmacotherapy as potent allies in addressing obesity (21,22).

Bariatric surgery encompasses diverse procedures, typically involving invasive alterations to stomach size/shape or intestinal passage to enhance weight loss (23). Such interventions should be reserved for cases of morbid obesity in adults due to associated complications and potential reoperations. Nevertheless, they deliver effective weight loss outcomes, ameliorating obesity-related comorbidities and enhancing overall patient quality of life (24).

On the pharmaceutical front, several compounds are available for obesity treatment, including orlistat (Xenical), naltrexone/bupropion (Contrave), phentermine/topiramate (Qsymia), liraglutide (Victoza) and tirzepatide (Mounjaro) (25,26). Orlistat, or Xenical as it is commercially known, is a synthetic lipase inhibitor akin to lipstatin, a natural lipase, first discovered in *Streptomyces toxytricini* bacteria (27). Orlistat selectively inhibits gastrointestinal lipases, reducing intestinal digestion and fat absorption, which results in weight reduction and improved cardiometabolic parameters such as lower insulin resistance and low-density lipoprotein (LDL) cholesterol levels (25). However, despite its low probability of causing adverse effects, it can cause diarrhoea and abdominal pain, as well as reduced absorption of some fat-soluble vitamins such as vitamins A, D, E, and K, making it contraindicated for patients with cholestasis or other kidney and/or liver problems (25,28). Contrave is a medicine that combines an opioid antagonist (naltrexone) with a norepinephrine and dopamine reuptake inhibitor (bupropion). This combination elevates pro-opiomelanocortin neuropeptide levels in the hypothalamus, resulting in a reduction of appetite and an increase in energy expenditure (25). However, it might lead to headaches or nausea and, in individuals with alcohol or opioid dependence, may trigger neuropsychiatric complications (25,29). Qsymia is also composed of two drugs: a norepinephrine stimulant (phentermine) and an anticonvulsant (topiramate) that can inhibit the activity of neurons involved in regulating appetite. This blend aids weight loss through appetite suppression, yet it may lead to cause nausea, and diarrhoea, and also may lead to depressive states (25,30). Liraglutide, the commercial Victoza, is an agonist of glucagon-like peptide-1 (GLP-1) receptors, resulting in an apparent increase in GLP-1

levels. This hormone is produced in the intestine and serves as a signal for reducing appetite and increasing energy expenditure. Furthermore, liraglutide stimulates insulin production in the pancreas, lowering blood sugar levels, while its administration also may trigger nausea, vomiting, and diarrhoea. Additionally, the recently approved tirzepatide, also an agonist of GLP-1 receptors, was the first drug to achieve close to or even above 20% weight loss, reported in a clinical trial with more than 2500 adults published in 2022 (31). However, some studies also associate GLP-1 receptor agonists with specific cancer types such as thyroid cancer (25,32).

The intricate metabolic nature of obesity justifies a comprehensive approach, considering the potential consequences of targeting adipocyte proliferation or adipogenesis, since such interventions, while aiming to combat obesity, could inadvertently trigger disorders like NAFLD, T2DM, and atherosclerosis. Moreover, excessive lipid degradation – lipolysis – may contribute to dyslipidaemia through elevated circulating fatty acids (33,34). Given the potential side effects of existing drugs used in the treatment of obesity, the urgency to identify safer and more effective alternatives becomes evident. Research and drug development efforts are thus intensifying, exploring novel compounds from both synthetic and natural sources. Recent investigations reveal a plethora of bioactive properties within crude extracts and isolated compounds, including secondary metabolites. These substances, sourced from diverse organisms like plants, fungi, and cyanobacteria, hold potential not only for combating obesity but also for addressing a broad spectrum of other medical conditions (2,24,34–37).

1.3 Harnessing Nature's Potential: Natural Products

Throughout the course of millennia, diverse cultures and civilisations have harnessed the healing potential of numerous plants and fungi, incorporating them into medicinal practices (38,39). Despite the persistence of this empirical tradition, a comprehensive understanding of the fundamental mechanisms behind their efficacy remained elusive. However, a pivotal advancement in elucidating the therapeutic attributes of these natural products (NPs) emerged during the 19th century with the isolation and commercialisation of morphine, a narcotic analgesic extracted from the opium poppy, *Papaver somniferum* (40,41). This seminal milestone not only marked a pioneering stride in unravelling the curative virtues inherent to nature's offerings but also underscored the historic role that plants and fungi had long assumed in nurturing human well-being. Yet, it was not until the 20th century that a groundbreaking

revelation, attributed to the scientist Alexander Fleming, would redirect scientific attention towards an alternative source of bioactive NPs – microorganisms. The discovery of penicillin, a momentous accomplishment made by chance, reshaped the landscape of pharmaceutical exploration, catalysing a heightened exploration of microbial reservoirs for novel therapeutic agents (42).

NPs can be delineated as the primary or secondary metabolites synthesised by living organisms (43). Nowadays, their potential in the treatment of obesity is being explored. This exploration arises from concerns regarding the high expenses and potentially hazardous side effects associated with current anti-obesity medications available in the market, as mentioned above. However, the investigation of these new compounds does not exempt them from undergoing an extensive safety testing phase.

NPs with anti-obesity properties can be systematically classified based on their molecular mechanisms into seven distinct groups: (i) lipase inhibitors, (ii) appetite suppressants, (iii) energy expenditure stimulants, (iv) adipocyte differentiation inhibitors, (v) lipogenesis inhibitors, (vi) lipolysis enhancers, and/or (vii) gut microbiota modifiers (36,44–46). Prior investigations have highlighted the potential of numerous phytochemicals that can be employed as anti-obesity agents, including polyphenols (e.g. resveratrol, curcumin, and catechins), alkaloids (e.g. capsaicin and ephedrine), and terpenoids (e.g. lycopene, abscisic acid) (46–49). Additionally, a new group of compounds has emerged and gained significance for their bioactivities against obesity – the chlorophyll derivatives (50,51). What lends relevance to these compounds is not solely their bioactivities, but also their derivation from a diverse array of natural sources, like plants, algae, and cyanobacteria.

1.4 Cyanobacteria: A Fascinating Phylum

Cyanobacteria are a phylum of gram-negative bacteria capable of carrying out photosynthesis, facilitated by chlorophyll a (52). While not exclusive to cyanobacteria, this ability plays a crucial role in their ecological significance once they show a high impact on carbon and oxygen cycles. Beyond their autotrophic nature, they wield a pivotal influence over the Earth's atmosphere composition. Furthermore, certain strains are also capable of fixing nitrogen, making them one of the most ecologically relevant groups of organisms on Earth (53).

The versatility of these organisms is truly striking, as they flourish across diverse environments, being found both in the fresh waters of the Amazon River and in

the hypersaline waters of the Dead Sea (54). Astonishingly, they also establish symbiotic relationships with organisms such as plants, animals, and other protists (55). As if that does not make them fascinating enough, many cyanobacteria have or can produce specialised cells such as heterocysts (nitrogen-fixing cells), akinetes (akin to spore-like dormant cells), and hormogonia (involved, amongst other roles, in reproduction) (56–58). Depending on the species, they can be categorised as unicellular, filamentous, or colonial. Concurrently, genetic analyses are being harnessed to untangle their intricate taxonomy. Notably, the most up-to-date cyanobacterial classification system has been elucidated by Strunecký *et al.* in 2023. This system employs a polyphasic phylogenomic approach, culminating in the proposition of ten novel orders and also fifteen new families (59).

However, despite their captivating attributes, cyanobacteria can exert adverse effects on ecosystems and human health, either due to algal blooms, an outcome of eutrophication in marine or riverine environments, or due to the production of toxins (60,61). Fortunately, these organisms also yield a variety of bioactive compounds that can be employed in the pharmaceutical, nutraceutical, and food industries (62).

1.4.1 Spirulina

Spirulina stands as one of the most widely consumed cyanobacteria globally. Its prevalence across diverse cultures has etched its name firmly into the lexicon of dietary choices. The nomenclature “spirulina” persists not merely for its phonetic convenience but also due to historical continuities, even as its taxonomic classification has undergone by revisions (63). In fact, spirulina serves as a common name encompassing various commercially relevant cyanobacterial species of the *Arthrospira* genus, like *A. platensis, A. maxima, A. fusiformis,* and *A. indica* (64). Notwithstanding, the nomenclature debate extends to the potential creation of a new genus, *Limnospira*, proposed by Nowicka-Krawczyk *et al.*, in 2019, to separate these species from the broader *Arthrospira* genus. Morphologically, these cyanobacteria are unicellular entities, with a width ranging between 6 and 8 μm wide and a length spanning from 2.6 to 5.6 μm. They congregate in filamentous colonies. Each filament – trichomes – is isopolar, cylindrical, spirally coiled or straight, and is composed of several single cells congregated. Within natural ecosystems, these organisms can assume benthic mat formations in temperate zones (64). Characterised by an elevated nutritional profile, spirulina emerges as being highly rich in protein and other macronutrients, as well as vitamins, minerals, and phytochemicals, including chlorophyll a (65).

Spirulina's safety for human consumption is underscored by both empirical evidence and the long-standing tradition of its incorporation into dietary customs, and consequently, spirulina was assigned the generally regarded as safe (GRAS) status for human consumption by the competent authorities such as Food and Drug Administration (FDA) and European Food Safety Authority (EFSA) (66–68). Some of their properties have been known empirically for a long time, however, recent studies have brought to light the mechanisms of action that explain the popular tradition of spirulina consumption. In a review published in 2020 by DiNicolantonio *et al.*, some bioactivities were highlighted that support its pharmaceutical and nutraceutical relevance. These included: anti-inflammatory properties, aid in weight loss due to the ability to inhibit pancreatic lipases and improve satiety. It has also shown abilities to regulate cholesterol levels as it promotes its excretion and improves dyslipidaemia (69). This makes spirulina an excellent source of NPs such as chlorophylls and their derivatives.

1.5 Chlorophyll derivatives: The Emerging Candidates

Chlorophylls are natural pigments biosynthesised by photosynthetic organisms such as plants, algae, and cyanobacteria (70,71). These photosynthetic pigments are involved in the capture of light energy. There are several types of chlorophylls, but the two most abundant types in nature are chlorophyll a and b in the ratio of 3:1, respectively (71). Structurally, both chlorophyll a and b have a cyclic tetrapyrrole. Each pyrrole ring is linked with methine bridges (–C=), and the four nitrogen atoms are linked to a central magnesium atom. In addition, there is also a fifth isocyclic ring and monounsaturated isoprenoid alcohol (phytol) esterified to the propionic acid tail in both chlorophylls. However, these molecules differ in position C–7, where chlorophyll a has a methyl group (–CH3), while chlorophyll b has a formyl group (–CHO) (Figure 1) (71).

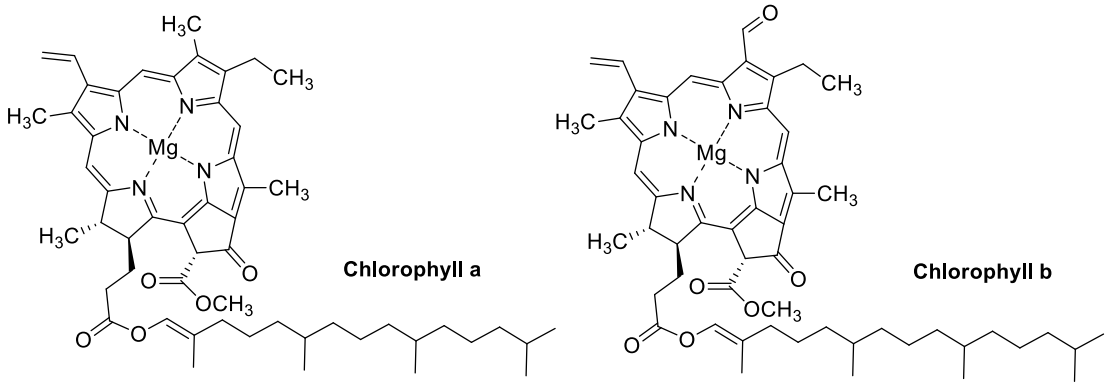

Figure 1 – **Chlorophylls chemical structures.** Chlorophyll a (left) and b (right).

Despite the structural similarity, only chlorophyll a is present in cyanobacteria (72). As mentioned above, spirulina has a high content of chlorophyll a, which makes it a reliable source of this molecule and its derivatives.

Chlorophyll a stability depends on processing and storage conditions such as pH, temperature, oxygen, metals, and enzymes. When exposed to extreme conditions, this sensitive molecule can undergo structural modifications, which can result in chlorophyll derivatives such as pheophytins, pyropheophytins, chlorophyllides, pheophorbides, and pyropheophorbides as illustrated in Figure 2. The three most common modifications are the loss of (i) magnesium centre, (ii) carbomethoxy group ($COOCH_3$), and/or (iii) phytol tail. Pheophytin a can emerge from chlorophyll a that loses its magnesium centre under acidic, heat, and/or enzymatic conditions. Furthermore, pyropheophytin a can be formed by long periods of heat degradation, however, both pheophytin a and pyropheophytin a are characterised by retaining their phytol tail but without the magnesium atom in the centre of the cyclic tetrapyrrole ring. On the other hand, phytol tail can be lost due to the action of chlorophyllase, a natural enzyme that catalyses its removal in a range of temperatures between 60 ºC and 82.2 ºC (71), originating chlorophyllide a from chlorophyll a and pheophorbide a from pheophytin a. Like pyropheophytin a, pyropheophorbide a can be formed by heat degradation, in the latter case, by heat degradation of pheophorbide a.

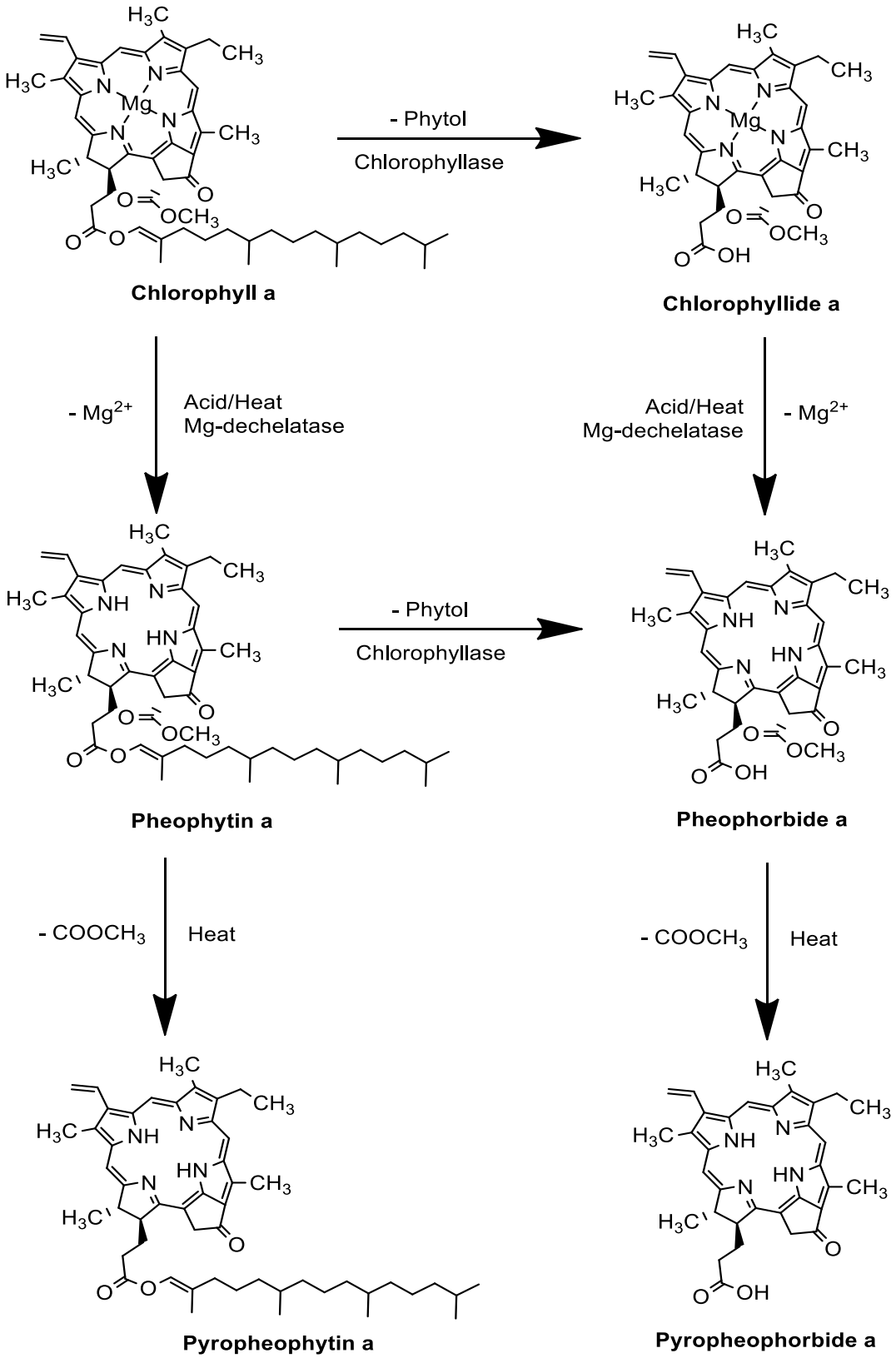

Figure 2 – **Chlorophyll a and its derivatives.** Relationship between the degrading conditions of chlorophyll a and its derivatives pheophytin a, pyropheophytin a, chlorophyllide a, pheophorbide a, and pyropheophorbide a. Adapted from Yilmaz *et al.* (71).

Chlorophyll derivatives have sparked scientific curiosity due to their various bioactivities such as antimicrobial, anti-inflammatory, and antioxidant which can be used for several medical purposes (73,74). Notably, they are also being investigated for their ability to be used in cancer therapies, such as photodynamic therapy, where they can act as photosensitizers (75,76). Regarding their application to treat obesity, there are still many gaps in knowledge. However, some derivatives with lipid-reduction and anti-adipogenic activities have been previously isolated and characterised. 13^2–hydroxy–pheophytin a and 13^2–hydroxy–pheofarnesin a reduced the neutral lipid reservoirs in zebrafish larvae (50), while pheophorbide a and pyropheophorbide a showed anti-adipogenic activities against differentiated adipocytes (77). Thus, compounds like these may be developed into future anti-obesity drugs and/or nutraceuticals.

1.6 Zebrafish: A Model Organism

To comprehend the capabilities and practical applicability of NPs, extracts, and pharmaceutical agents, a fundamental prerequisite involves a comprehensive determination of their bioactivity. While a fully autonomous *in silico* approach for this purpose is lacking, empirical *in vivo* models remain indispensable tools for investigating various human ailments. A variety of techniques and methodologies can be harnessed to evaluate the efficacy of compounds in the context of combating obesity. Ranging from assays that reduce appetite to those that inhibit lipid absorption, an array of alternative methodologies can be employed to discern the potential anti-obesity effects, whether within *in vitro* environments or through *in vivo* experimentation. *In vitro* assays, however, while offering improved reproducibility and quicker results, do not entirely encapsulate the intricate physiological interactions inherent in living organisms, which are crucial to the study of obesity. Furthermore, certain compounds that exhibit utility *in vitro* often fail to exhibit comparable effectiveness *in vivo* or may even engender undue toxicities.

Given these limitations and challenges inherent in cellular models, smaller whole-animal models present themselves as alternative avenues. Particularly noteworthy is the zebrafish (*Danio rerio*), a diminutive freshwater teleost, which has gained substantial acclaim and prominence as a model organism in the realm of biomedical research due to its high degree of genetic, anatomical, and physiological similarities to humans. Notwithstanding their phylogenetic divergence from humans, zebrafish possess nervous and endocrine systems that evoke a noteworthy

physiological semblance to humans, allowing their use as model organisms in the study of metabolic diseases such as obesity. However, zebrafish is an ectotherm species and its metabolic rate is regulated by environmental temperature. Consistent with this, zebrafish do not have BAT (78). Despite that, these animals exhibit a high fecundity, facile maintenance, and handling, and have a short life cycle. As oviparous beings, their transparent embryos undergo extracorporeal development. A common practice is to impede pigmentation approximately 1 to 2 days post fertilisation (DPF), thereby maintaining larval translucence. This characteristic trait permits the application of fluorescent markers as a screening method to scrutinise diverse biological processes and their associated pathologies (78,79).

1.7 Objectives

This dissertation has been developed at the Biodiscovery for Health research group, from the Interdisciplinary Centre of Marine and Environmental Research (CIIMAR). A primary focus of this research group resides in the exploration of cyanobacteria NPs with pharmaceutical and biotechnological applications, particularly for addressing metabolic diseases. Following the discovery of lipid-reducing activities of 13^2-hydroxy-pheophytin a, this work aimed to systematically investigate the extraction and modification of chlorophyll a derivatives from *A. platensis* and their anti-obesity activities.

The central objective of this study can be summarised into two main topics: first, it was determined which of the tested extraction methods was the most effective for extracting chlorophyll a derivatives. Second, the identification and evaluation of the potential of these compounds as viable candidates for obesity treatment was performed through a comprehensive analysis of their abilities to reduce lipids and appetite. To achieve these objectives, the following workflow was followed:

1. **Extractions:** Several extraction conditions were chosen and extraction were performed to determine the optimal approach for obtaining crude extracts enriched with chlorophyll a and its derivatives from *A. platensis* (spirulina) biomass.

2. **Characterisation of the lipid and appetite-reducing activities:** To assess the lipid-reducing efficacy of these crude extracts and their impact on appetite, two assays using zebrafish larvae were conducted: the zebrafish Nile Red fat metabolism assay and a liposome-based assay for appetite reduction.

3. **Metabolomic analysis by mass spectrometry:** Mass spectrometry techniques, along with molecular networks and *in silico* tools, were used to putatively identify compound present in bioactive extracts were .

Therefore, this study not only seeks to enhance the understanding of the potential of chlorophyll a and its derivatives as bioactive compounds for obesity treatment, but also aims to establish more efficient extraction protocols for these compounds.

2. Materials & Methods

2.1 Chemical Procedures

2.1.1 Organic Extractions

The first stage, chemical procedures, involved various extractions to obtain crude extracts enriched in chlorophyll a derivatives. At this part of the work, a group of prospecting extractions was conducted, followed by a group of targeted extractions to obtain extracts enriched in chlorophyll a derivatives. The targeted extractions were designed based on the prior analysis of the crude extracts from the prospecting extractions.

In order to obtain crude extracts enriched in chlorophyll a derivatives, approximately 28 g of commercially available spirulina (*A. platensis*) biomass (ISWARI™ Spirulina powder) were used as a chlorophyll a source. Four distinct analytical grade solvents were used: >99.8% methanol (VWR Chemicals), 96% ethanol (PanReac AppliChem ITW Reagents), >99% acetone (VWR Chemicals), and 99.8% dichloromethane (Fisher Chemical™). All solvents, except for 99.8% dichloromethane, were diluted in ultrapure water (UPW) to achieve the intended final concentrations. These were 90% methanol (MeOH/H_2O, 9:1, v/v), 70% ethanol (EtOH/H_2O, 7:3, v/v), and 90% acetone (CH_3COCH_3/H_2O, 9:1, v/v). A Bandelin Sonorex RK100H sonicator was used to disrupt cellular structures, while subsequent solvent evaporation from the crude extracts was undertaken via a Rotavapor R–300 (BUCHI) under variable reduced pressure according to solvent with Vacuum Pump V–300 (BUCHI) using Recirculating Chiller (BUCHI) at - 8 ºC with sample maintained in Heating Bath B–300 Base (BUCHI) at 30 °C, following filtration. Prior to storage at - 20 ºC, all vials were weighed before and after extract introduction using a Sartorius™ Secura™ analytical balance, identified, and sealed with parafilm.

The twenty-eight performed extractions were systematically organised into 8 sets. Sets 1 to 4 constituted the preliminary prospecting extraction group, whereas sets 5 to 8 were performed after the prospecting group, focusing on more targeted extraction strategies. The RGB colour codes were collected from a picture of each extract diluted in DMSO (0.1%) and using the ImageJ 1.53a program. These RGB codes were used to make the different colours of the extracts graphically visible.

2.1.1.1 Prospecting Extractions

In the 16 prospecting extractions, the four previously mentioned solvents were used, alongside variations in extraction temperatures, sample sonication, and post-extraction acidification. This iterative approach led to the formulation of four distinct sets, each encompassing a quartet of extractions.

For set 1, the protocol involved combine 1 g of spirulina biomass with 160 mL of each one of the four previously mentioned solvents, separately. This mixture was then subjected to a 10-minute sonication followed by an extraction cycle with constant agitation lasting 2 hours and 50 minutes, both at room temperature (22 °C). All the protocol was conducted in a light-free environment, obtained by covering the mixture with aluminium foil. This process yielded the production of crude extracts denoted as M1, E1, A1, and D1 (as detailed in Table 1).

Set 2 adhered to the same procedural steps as set 1, but without the sonication step. Consequently, crude extracts M2, E2, A2, and D2 emerged as non-sonicated versions of the extracts derived from set 1.

In set 3, the mixture of 1 g of spirulina biomass and 160 mL of the designated solvent underwent 10 minutes of sonication, succeeded by an extraction duration of 2 hours and 50 minutes, executed under controlled heating conditions, and covered with aluminium foil. The selection of extraction temperature was premised on the boiling point intrinsic to each solvent and adjust to prevent the mixture from pumping into the condenser; thus, extraction temperatures for 90% methanol, 70% ethanol, 90% acetone, and 99.8% dichloromethane were 50°C, 60°C, 50°C, and 32.5°C, respectively. This yielded the extraction outcomes of M3, E3, A3, and D3. To obviate the solvent evaporation, a closed system was implemented, comprising a reflux condenser for solvent condensation, a nitrogen (N_2) rubber balloon to preserve an inert milieu, a 250 mL volumetric flask for mixture containment, and an Electrothermal EM250 heating mantle for temperature regulation during extraction, as illustrated in Figure 3.

Lastly, set 4 retained the extraction procedure of set 1, but introduced a post-treatment exposing the crude extracts to hydrochloric acid (HCl) (Acros Organic Hydrochloric Acid, 0.1 N) at a final concentration of 0.008 M for 1 hour. This resulted in the production of M4, E4, A4, and D4.

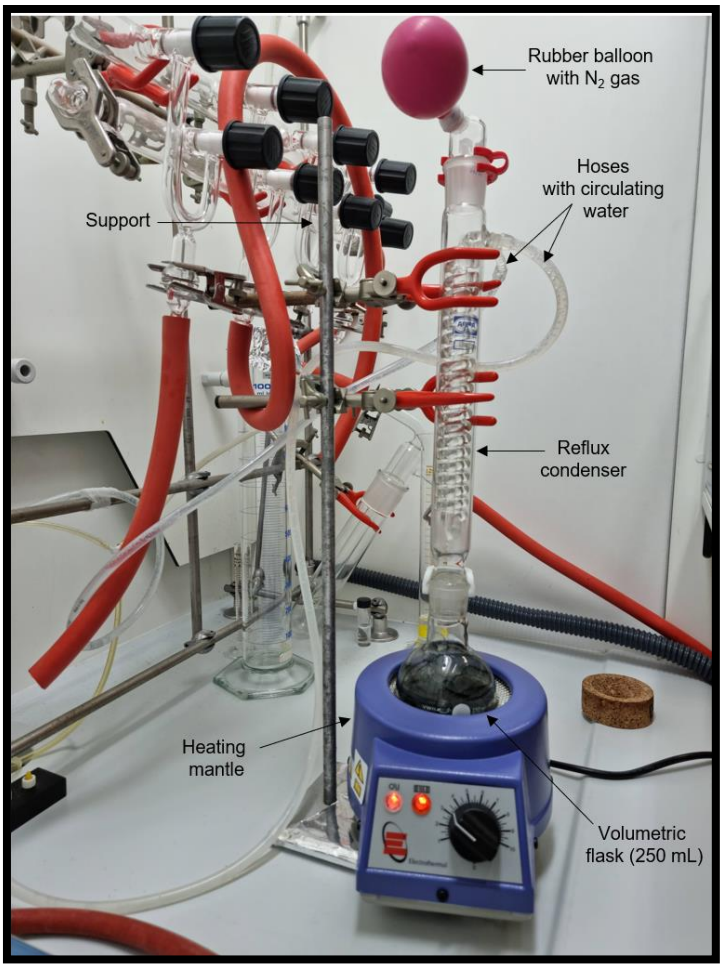

Figure 3 – **Extraction under reflux setup.** The volumetric flask was covered with aluminium foil despite it not being shown in the representation.

Table 1 – **Extraction details of prospective extraction sets.**

Set	Code	Spirulina biomass	Solvent	Overall time	Pre-treatment	Extraction	Post-treatment
1	M1	1.03 g	160 mL MeOH/H2O (9/1, v/v)	**3h**	10 '' sonication (dark + 22 ºC)	2h50'' agitation (dark + 22 ºC)	-
	E1	1.07 g	160 mL EtOH/H2O (7/3, v/v)	**3h**	10'' sonication (dark + 22 ºC)	2h50'' agitation (dark + 22 ºC)	-
	A1	1.01 g	160 mL CH_3COCH_3/H2O (9/1, v/v)	**3h**	10'' sonication (dark + 22 ºC)	2h50'' agitation (dark + 22 ºC)	-
	D1	1.07 g	160 mL CH_2Cl_2	**3h**	10'' sonication (dark + 22 ºC)	2h50'' agitation (dark + 22 ºC)	-
2	M2	1.00 g	160 mL MeOH/H2O (9/1, v/v)	**3h**	-	3h agitation (dark + 22 ºC)	-
	E2	1.04 g	160 mL EtOH/H2O (7/3, v/v)	**3h**	-	3h agitation (dark + 22 ºC)	-
	A2	1.03 g	160 mL CH_3COCH_3/H2O (9/1, v/v)	**3h**	-	3h agitation (dark + 22 ºC)	-
	D2	1.02 g	160 mL CH_2Cl_2	**3h**	-	3h agitation (dark + 22 ºC)	-
3	M3	1.01 g	160 mL MeOH/H2O (9/1, v/v)	**3h**	10'' sonication (dark + 22 ºC)	2h50'' in reflux (dark + 50 ºC)	-
	E3	1.04 g	160 mL EtOH/H2O (7/3, v/v)	**3h**	10'' sonication (dark + 22 ºC)	2h50'' in reflux (dark + 60 ºC)	-
	A3	1.03 g	160 mL CH_3COCH_3/H2O (9/1, v/v)	**3h**	10'' sonication (dark + 22 ºC)	2h50'' in reflux (dark + 50 ºC)	-
	D3	1.04 g	160 mL CH_2Cl_2	**3h**	10'' sonication (dark + 22 ºC)	2h50'' in reflux (dark + 32.5 ºC)	-
4	M4	1.00 g	160 mL MeOH/H2O (9/1, v/v)	**4h**	10'' sonication (dark + 22 ºC)	2h50'' agitation (dark + 22 ºC)	1h HCl (0.008 M), 22ºC
	E4	1.02 g	160 mL EtOH/H2O (7/3, v/v)	**4h**	10'' sonication (dark + 22 ºC)	2h50'' agitation (dark + 22 ºC)	1h HCl (0.008 M), 22ºC
	A4	1.03 g	160 mL CH_3COCH_3/H2O (9/1, v/v)	**4h**	10'' sonication (dark + 22 ºC)	2h50'' agitation (dark + 22 ºC)	1h HCl (0.008 M), 22ºC
	D4	1.01 g	160 mL CH_2Cl_2	**4h**	10'' sonication (dark + 22 ºC)	2h50'' agitation (dark + 22 ºC)	1h HCl (0.008 M), 22 ºC

2.1.1.2 Targeted Extractions

In the 12 targeted extractions, the aim was to obtain extracts enriched in more degraded chlorophyll a derivatives, such as pyropheophytin a and pyropheophorbide a. These extracts were categorised into four distinct extraction sets – 5, 6, 7, and 8 – each one comprising three individual extracts.

In all extraction sets, approximately 1 g of biomass was subjected to water decoction within 160 mL of UPW. The specific decoction temperatures employed were 80 ºC for sets 5 and 7, and 100 ºC for sets 6 and 8. The water levels were maintained by several addictions, since its evaporation was inevitable. After the decoction, the

volume of the mixture was measured and adjusted to 160 mL and the EtOH was adjusted to the final concentration of 70% EtOH. Following this EtOH adjustment, the mixture underwent a 10 min sonication step, followed by a subsequent period of gentle agitation for 2 h 50 min at 22 ºC and covered with aluminium foil.

For sets 7 and 8, the extraction protocols closely mirrored those of sets 5 and 6, respectively. Notably, an additional phase was introduced wherein the mixture was treated with 0.08 M HCl for a duration of 1 hour at 22 ºC. This supplementary step occurred prior to the ethanol addiction and the subsequent 2 h 50 min of stirring, also covered with aluminium foil, and performed at 22 ºC.

A total of 12 extraction procedures were conducted, yielding twelve crude extracts designated as detailed in Table 2.

Table 2 – **Extraction details of targeted extraction sets.**

	Code	Spirulina biomass	Solvent	Overall time	Pre-treatment	Extraction
5	E5a	1.03 g	160 mL EtOH/H2O (7/3, v/v)	**4h**	1h UPW decoction (160 mL), 80ºC + 10'' sonication, 22 ºC	2h50'' agitation (dark + 22 ºC)
	E5b	1.02 g	160 mL EtOH/H2O (7/3, v/v)	**5h**	2h UPW decoction (160 mL), 80ºC + 10'' sonication, 22 ºC	2h50'' agitation (dark + 22 ºC)
	E5c	1.02 g	160 mL EtOH/H2O (7/3, v/v)	**7h**	4h UPW decoction (160 mL), 80ºC + 10'' sonication, 22 ºC	2h50'' agitation (dark + 22 ºC)
6	E6a	1.01 g	160 mL EtOH/H2O (7/3, v/v)	**4h**	1h UPW decoction (160 mL), 100ºC + 10'' sonication, 22 ºC	2h50'' agitation (dark + 22 ºC)
	E6b	1.01 g	160 mL EtOH/H2O (7/3, v/v)	**5h**	2h UPW decoction (160 mL), 100ºC + 10'' sonication, 22 ºC	2h50'' agitation (dark + 22 ºC)
	E6c	1.01 g	160 mL EtOH/H2O (7/3, v/v)	**7h**	4h UPW decoction (160 mL), 100ºC + 10'' sonication, 22 ºC	2h50'' agitation (dark + 22 ºC)
7	E7a	1.02 g	160 mL EtOH/H2O (7/3, v/v)	**5h**	1h UPW decoction (160 mL), 80ºC + 1h HCl 0.08 M, 22 ºC + 10'' sonication, 22 ºC	2h50'' agitation (dark + 22 ºC)
	E7b	1.02 g	160 mL EtOH/H2O (7/3, v/v)	**6h**	2h UPW decoction (160 mL), 80 ºC + 1h HCl 0.08 M 22 ºC + 10'' sonication	2h50'' agitation (dark + 22 ºC)
	E7c	1.02 g	160 mL EtOH/H2O (7/3, v/v)	**8h**	4h UPW decoction (160 mL), 80ºC + 1h HCl 0.08 M, 22 ºC + 10'' sonication, 22 ºC	2h50'' agitation (dark + 22 ºC)
8	E8a	1.00 g	160 mL EtOH/H2O (7/3, v/v)	**5h**	1h UPW decoction (160 mL), 100ºC + 1h HCl 0.08 M, 22 ºC + 10'' sonication, 22 ºC	2h50'' agitation (dark + 22 ºC)
	E8b	1.00 g	160 mL EtOH/H2O (7/3, v/v)	**6h**	2h UPW decoction (160 mL), 100ºC + 1h HCl 0.08 M, 22 ºC + 10'' sonication, 22 ºC	2h50'' agitation (dark + 22 ºC)
	E8c	1.00 g	160 mL EtOH/H2O (7/3, v/v)	**8h**	4h UPW decoction (160 mL), 100ºC + 1h HCl 0.08 M 22 ºC + 10'' sonication, 22 ºC	2h50'' agitation (dark + 22 ºC)

2.2 Biological Procedures

2.2.1 Zebrafish Larvae Preparation

For the following assays, the same protocol of zebrafish larvae preparation was performed. On the day prior to fertilisation, zebrafish males were segregated from females. Subsequently, the males and females were put together within a confined aquatic environment mimicking coastal-river conditions, using a structure denominated as “sex on the beach”, under appropriate lighting to promote fish mating. Within 0 to 6 hours post fertilisation, zebrafish eggs were harvested and kept in 60 µg/mL sea salt medium (egg water). Nonviable eggs, dead eggs, eggshells, and faecal matter were discarded, while viable eggs were transferred to petri dishes containing E3 medium (composed of 5 mM NaCl, 0.17 mM KCl, 0.33 mM $CaCl_2$, 0.33 mM $MgCl_2$) supplemented with 1:10,000 dilution of 1% methylene blue (MB), a fungicidal agent. The dishes were maintained in an incubator at a temperature of 28 ºC. At 1 DPF, the medium was replaced and 1–phenyl–2–thiourea (PTU) was added at a final concentration of 200 µM to suppress larval pigmentation. Upon reaching 3 DPF, embryos and larvae were observed with a stereo microscope (Olympus SZX10) and separated according to their developmental stage and anomalies. Non-viable specimens were culled for euthanasia, while viable and healthy ones were used in the assays.

2.2.2 Zebrafish Nile Red Fat Metabolism Assay

The following protocol has been previously described by Freitas *et al.*, in 2019, with minor adaptations to minimise fungal infections (50). The assay spans a total duration of 5 days. Once the larvae were prepared and reached 3 DPF, four larvae were transferred to each well in a 96-well plate, containing E3 medium without MB and subjected to crude extracts diluted at a ratio of 1:1000 in dimethyl-sulfoxide (DMSO), resulting in a final exposure concentration of 10 µg/mL. Each well-plate also included three wells for both positive control resveratrol (REV, 50µM), a lipid reducing compound in zebrafish, and a solvent control, DMSO (0.1%). The well-plate was covered with aluminium foil to prevent the photodegradation of the components and incubated at 28 ºC. On 4 DPF a neutral lipid stain, Nile Red (NR), was added at a final concentration of 10 ng/mL. Finally, on 5 DPF, the larvae were anesthetised with 0.03% tricaine (MS–222, Sigma-Aldrich), and fluorescence intensities were read on the Cytation 5 image reader (BioTek Instruments Inc) using the Gen5 3.10 program. At least two independent assays were conducted during separate weeks to enhance the robustness of the data assay.

2.2.3 Liposome-based Assay for Appetite Reduction

The liposome-based assay encompasses a 7-day timeframe. The larvae were incubated until 5 DPF. Then, E3 medium was renewed, and larvae were fed twice on that day. At 6 DPF, a cohort of six to eight larvae was transferred to each well within a 48-well plate with E3. Larvae underwent a pre-treatment involving the administration of the extracts at 10 μg/mL for 24h. Each plate also included three wells for positive controls – fluoxetine hydrochloride (FLX, Sigma-Aldrich) – an appetite-suppressing agent, at a final exposure concentration of 10 mM. An additional three wells were used as solvent controls, featuring DMSO (0.1%). The well-plate was covered with aluminium foil and incubated at 28 ºC. Finally, on 7 DPF, a liposomes solution was prepared mixing an aliquot of egg yolk (1 mL) in 19 mL of E3 medium, followed by vacuum filtration using a 55 μm mesh filter. The filtrate was subjected to a series of 25 cycles of sonication in a Bandelin Sonopuls HD 2070.2 ultrasonic homogeniser. Each sonication cycle comprised five instances of 1-second pulses, interspersed with 5-second intervals. This sonication regime promoted the generation of liposomes, subsequently stained with BODIPY FL-C16 at a final exposure concentration of 6.4 μM. Within the 48-well plate, the E3 medium supplemented with the extracts and controls were meticulously aspirated and, subsequently, replaced by 750 μL of the stained liposome suspension into each well. The plate was covered with aluminium foil to prevent the photodegradation of the dye, and incubated for 2 hours at 28 °C. After the incubation, the liposome medium was thoroughly aspirated, and three successive washes with E3 medium were conducted. The zebrafish were transferred to a new 48-well plate and anesthetised with a 0.03% solution of MS-222. Subsequent fluorescence measurements were performed using an automated fluorescence microscope (Leica, Thunder imager), operating in conjunction with the LAS X microscope software (80,81). At least two independent assays were conducted during separate weeks to enhance the robustness of the data assay.

2.2.4 Data Analysis

The mean fluorescence intensity (MFI) was individually quantified in the ImageJ 1.53a program and normalised to solvent control (DMSO) mean value for both previous described assays. Statistical differences were analysed by GraphPad Prism 8 program. Gaussian distribution was tested by Kolmogorov-Smirnov test (p value < 0.05). One-Way ANOVA was used to analyse significant differences of the extracts compared to the solvent control group. Dunnett's post hoc test was used if data had a parametric distribution, while Kruskal-Wallis with Dunn's post hoc test was used if data had a non-

parametric distribution. The data were represented as box-whisker plots in 5 – 95 percentiles, and extracts with significance differences were noted by asterisks (* = $p < 0.05$, ** = $p < 0.01$, *** = $p < 0.001$).

2.3 Metabolomics Analysis

2.3.1 Mass Spectrometry Data Acquisition

All samples underwent analysis via the liquid chromatography-high-resolution electrospray ionisation tandem mass spectrometry (LC-HR ESI-MS/MS) technique performed at the Materials Centre of the University of Porto (CEMUP). This procedure was executed using a Vanquish™ high performance liquid chromatography (HPLC) system linked to an Orbitrap Exploris 120 mass spectrometer. The system was managed by Q Exactive Focus Tune 2.9 and Xcalibur 4.1 software (Thermo Fisher Scientific, Waltham, MA, USA). The analysis was conducted in full positive scan mode, employing specific parameters: the capillary temperature was set to 262.5 °C, the spray voltage was maintained at 3.5 kV, and a resolution of 70,000 FWHM was chosen for the mass-to-charge (*m/z*) ratio range of 150–2000. Additionally, a data dependent MS^2 ($ddMS^2$, Discovery mode) was performed at a resolution of 17,500 FWHM. This involved an isolation window of 3.0 amu and a normalised collision energy setting of 35. The sample extracts (5 µl; 2 mg/ml in MS-grade MeOH, Thermo Fisher Scientific) were separated by passing them through an ACE UltraCore 2.5 SuperC18 column (75 × 2.1 mm, ACE, Reading, UK) at a temperature of 40 °C. A gradient elution strategy was adopted, starting with a transition from 99.5% H_2O/MeOH/formic acid (95:5:0.1, v/v) to 10% over a span of 9.5 minutes. Subsequently, there was a transition from 0.5% to 90% isopropanol/MeOH/formic acid (95:5:0.1, v/v) until 15.5 minutes. The final mixture was held for 15.5 minutes before reverting to the initial conditions. Throughout this process, the flow rate was maintained at 0.35 mL/min.

Once the LC-HR ESI-MS/MS raw data were obtained, the presence of chlorophyll a and selected derivatives were evaluated by comparison of obtained MS^2 spectra and predicted ones using the competitive fragmentation modelling for metabolite identification (CFM-ID, https://cfmid.wishartlab.com/) (82). Peak areas were annotated in Xcalibur 4.1 software for compounds that showed ppm mass error values lower than 5. These data were synthesised in two heatmaps made using Plotly Chart Studio (https://chart-studio.plotly.com/feed/#/) (83).

2.3.2 Molecular Network

The raw LC-HR ESI-MS/MS data were converted into the .mzML format using the MSconvertGUI 3.0 tool from ProteoWizard software package. Subsequently, the .mzML files were uploaded to the global natural products social molecular networking (GNPS; http://gnps.ucsd.edu) platform using the WinSCP 5.21.7 program. A molecular networking approach (METABOLOMICS-SNETS-V2) was performed at GNPS. Both precursor ion and fragment ion mass tolerance were set at 0.02 Da. During this process, edges were subjected to a cosine score threshold of above 0.7 and required a minimum of 6 matched peaks. Furthermore, edges connecting two nodes were retained in the network solely if each node appeared in the respective top 10 most similar nodes of the other. The maximum size for a molecular family was capped at 100, and the lowest-scoring edges were systematically removed from molecular families until the size of a given molecular family fell below this threshold. In the network, spectra were subsequently cross-referenced against GNPS spectral libraries. Matches between network spectra and library spectra necessitated a score surpassing 0.7 and the presence of at least 6 matched peaks. For optimisation of chemical structural information within the molecular networks, insights from *in silico* structure annotations stemming from GNPS Library Search, Network Annotation Propagation (NAP) (84), DEREPLICATOR (85), and MS2LDA (86) were incorporated. This incorporation was achieved through the GNPS MolNetEnhancer workflow (87), accessible via the GNPS website (88). This workflow was applied to both extraction groups: prospective and targeted extractions. To visualise the molecular networks, the Cytoscape 3.9.1 software was employed (89). This software enabled the annotation of compound families and the visualisation of unique compounds only present in bioactive crude extracts. Notably, the blank runs were filtered prior to the networking process, to remove false positives.

3. Results

3.1 Extractions

Overall, the extractions were successful, and 28 extracts were obtained (Figures 4A and 4B) and the amount of extract was counted (Figures 4C and 4D).

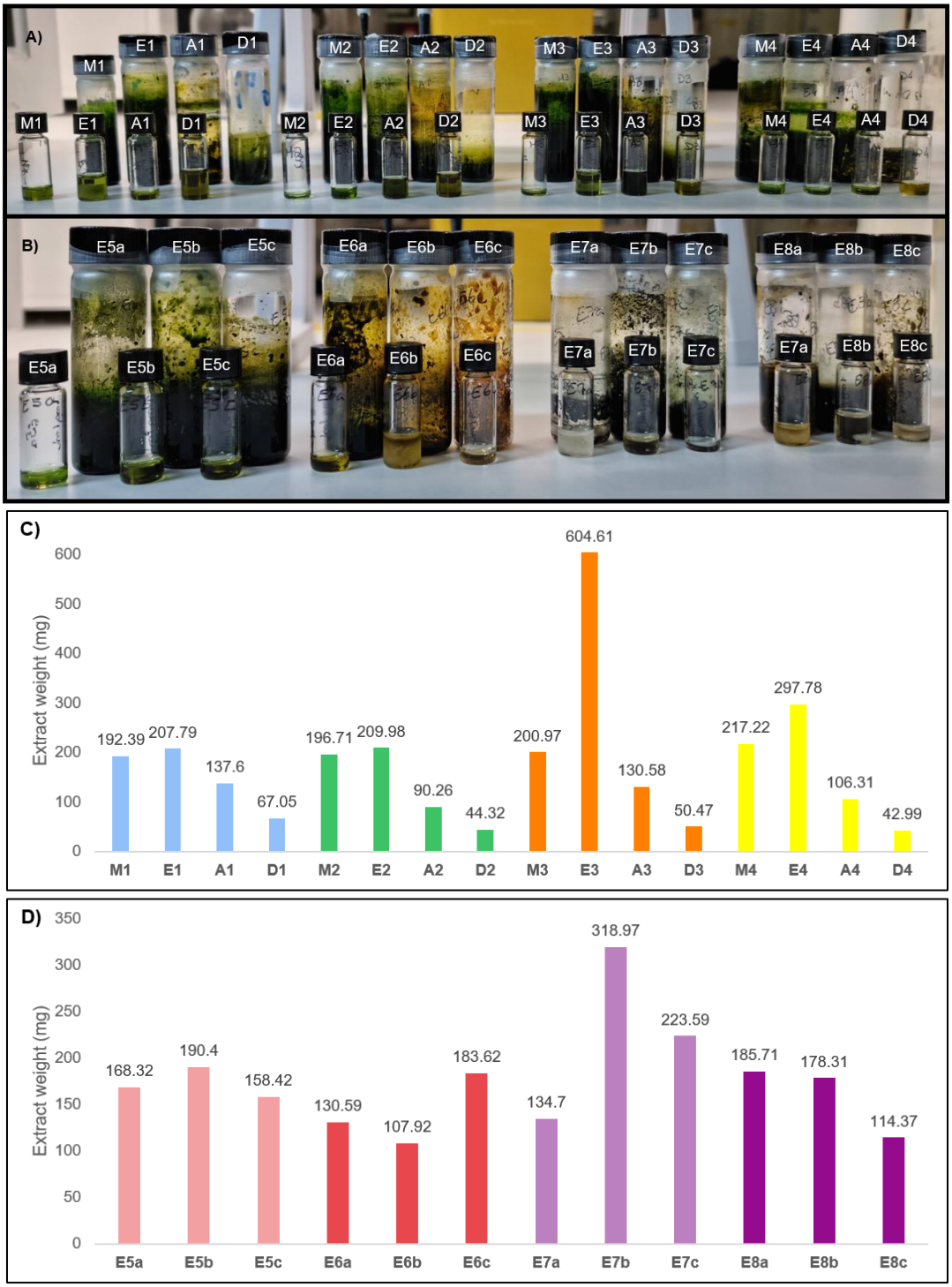

Figure 4 – **Spirulina crude extracts.** Dry extracts (background) and extracts at 1 mg/mL in DMSO (foreground) from prospecting extractions (A) and targeted extractions (B). Weight of prospecting (C) and targeted extracts (D).

The extractions where dichloromethane was used (D1, D2, D3, and D4) were responsible for the lowest amount of extract, followed by extractions with 90% acetone (A1, A2, A3, and A4) (Figure 4C). The extractions with 70% ethanol (E3, E4, E2, and E1) produced the highest amount of extract, followed by methanolic extractions (M4, M3, M2, M1). E3 and E7b extractions produced the highest amount of extract, 604.61 mg, and 318.97 mg, respectively, from 1 g of spirulina biomass (Figure 4C and 4D).

Table 3 – **RGB colour codes of the extracts.**

Crude extract	RGB code
M1	#3d4907
E1	#5a6306
A1	#7b761b
D1	#695e02
M2	#97a567
E2	#2a400f
A2	#44480d
D2	#4e4208
M3	#838c3b
E3	#71781b
A3	#13190d
D3	#4f4605
M4	#4E6713
E4	#69733e
A4	#585d0d
D4	#4a3a06
E5a	#495E19
E5b	#5B6310
E5c	#625C10
E6a	#5C4C19
E6b	#86670c
E6c	#a5986c
E7a	#a49d8b
E7b	#8f7b46
E7c	#736F63
E8a	#7d6122
E8b	#9b8c75
E8c	#887743

Concerning the extracts colours, they were relatively uniform between extraction groups (Table 3). Prospecting extractions showed several shades of green, where the A3 were the extract that presented a darker colour, as can be seen in both Figure 4A and Table 3. For targeted extractions, a variety of greens, browns and greys were observed (Figure 4B and Table 3), which was an indicator of chlorophyll a degradation since this molecule has a bright green colour while derivatives such as pheophytins and pyropheophytins have a yellow-brown olive colour (90).

3.2 Relative Quantification of Chlorophyll a and Its Derivatives by High Resolution Mass Spectrometry

The targeted metabolomic analysis by LC-HR ESI-MS/MS was used to assess the effect of the different extraction methods on the yields of chlorophyll a and its derivatives. The peak area of the protonated ions of chlorophyll a, chlorophyllide a, pheophytin a, 13^2-hydroxy-pheophytin a, pyropheophytin a, pheophorbide a, and pyropheophorbide a were noted for each compound in each extract. The accurate masses were obtained from PubChem, in 2023 (91), with the subsequent addition of a the exact mass of hydrogen [H^+=1.00784 Da]. MS^2 spectra were predicted using the CFM-ID (82) to compare to the obtained ones. The adducts were also verified through known *m/z* differences and isomers were also found. Additionally, a mass error was calculated, expressed in parts per million (ppm). Peaks areas were considered when the mass error was less than 5 ppm. Table 4 summarises the presence of selected compounds and founded isomers in different extracts. Additionally, mean retention time (Rt), calculated *m/z* $[M+H]^+$, mean experimental *m/z* $[M+H]^+$, and mass error were noted. The raw data are found in Table S1.

Table 4 – **Summary of the expected chlorophyll a and its derivatives in the extracts.** Mean values of retention time (Rt), experimental *m/z* $[M+H]^+$, and mass error.

Compound	Rt (min)	Calculated *m/z* $[M+H]^+$	Experimental *m/z* $[M+H]^+$	Mass error (ppm)	Detected in
Chlorophyll a	13.17	893.5431	893.5413	2.0737	A2, D2, D3 and D4
Chlorophyll a'	13.39	8935431	893.5413	2.0737	D1, D3 and D4
Chlorophyllide a	-	615.2458	-	-	None
Pheophytin a	14.05	871.5737	871.5719	2.1352	All extracts
Pheophytin a'	14.30	871.5737	871.5717	2.3646	All extracts except E2 and E6c
13^2-hydroxy-pheophytin a	13.67	887.5697	887.5664	3.7180	All extracts except E2
13^2-hydroxy-pheophytin a'	13.82	887.5697	887.5666	3.4926	All extracts except E2
Pyropheophytin a	14.88	813.5677	813.5661	1.9666	Only in targeted extractions
Pyropheophytin a'	15.18	813.5677	813.5666	1.3520	Only in prospecting extractions
Pheophorbide a	11.20	593.2764	593.2752	2.0412	Only in targeted extractions
Pheophorbide a'	11.30	593.2764	593.2751	2.2097	A2, E3, set 7, and set 8
Pyropheophorbide a	11.70	535.2709	535.2696	2.4865	Only in targeted extractions

The relative detection of the different analysed compounds was based on peak area annotations, and the data were organised in a general heatmap (Figure 5). Additionally, another heatmap was generated to allow the better visualisation of low relative abundant selected compounds (Figure 6).

Thus, chlorophylls (chlorophyll a and chlorophyll a') were poorly detected even in the prospective group (Figure 6). However, extractions with dichloromethane proved to be the most suitable for extracting this pigment and its isomer, particularly extractions D3 (where the extraction temperature was 32.5ºC, Table 1) and D4 (post-treatment with a low concentration of HCl, Table 1). Additionally, chlorophyll a was also detected in extracts A2 and D2, while chlorophyll a' was also detected in D1. Chlorophyllide a was not detected in any of the extractions performed, while pheophytins (pheophytin a, pheophytin a', 13^2-hydroxy-pheophytin a, and 13^2-hydroxy-pheophytin a') were the most detected derivatives, showing a greater relative abundance in both prospective and targeted extractions. Accordingly, pheophytin a was detected in all extracts, but higher peak areas were found in E8a, E3, E5b, and E5c extracts. Its isomer, pheophytin a', was detected in greater relative abundance in E5a and was also present in all extracts, except for E2 and E6c. Extract E2 was the only one where neither 13^2-hydroxy-pheophytin a nor its isomer 13^2-hydroxy-pheophytin a' were detected. However, high peak areas of 13^2-hydroxy-pheophytin a were detected in E5b, M1, E4, and M4 extracts, while its isomer was detected in greater relative abundance in A2, A1, and E5a extracts. In the extraction of pyropheophytins, a separation was observed, with pyropheophytin a only being detected in targeted extractions, while its isomer, pyropheophytin a', was only detected in prospective extractions, except for E2 and D2. Compared to pheophytins, these pyro-derivatives were less detected in the extracts. Nevertheless, E6b and E8c proved to be the best choices for obtaining extracts enriched in pyropheophytin a. Its isomer had the highest peak area values in D4. Regarding pheophorbides, in most of the extracts, none of the isomers were detected. The detection of pheophorbide a occurred only in targeted extractions, except in E5c and E6c. E7a and E8a extracts were the most effective in extracting/producing this derivative. Its isomer was detected in only 6 of the 28 extracts (A2, E3, E7a, E7b, E7c, E8a, and E8b), with A2 being the extract where this isomer showed the highest peak area. Finally, pyropheophorbide a was only detected in targeted extractions (similar to pyropheophytin a and pheophorbide a), with extraction E8b being the most effective in producing an extract enriched in this chlorophyll a pyro-derivative.

In summary, chlorophylls were barely detected, while pheophytins were ubiquitously extracted, detected in most of the extracts. Pheophorbides (pheophorbide a and pheophorbide a') were more effectively extracted by targeted extractions, except for the isomer pheophorbide a', which was highly detected in A2. Chlorophyll a pyro-

derivatives (pyropheophytin a, pyropheophytin a', and pyropheophorbide a) were more effectively obtained in targeted extractions (Figure 6).

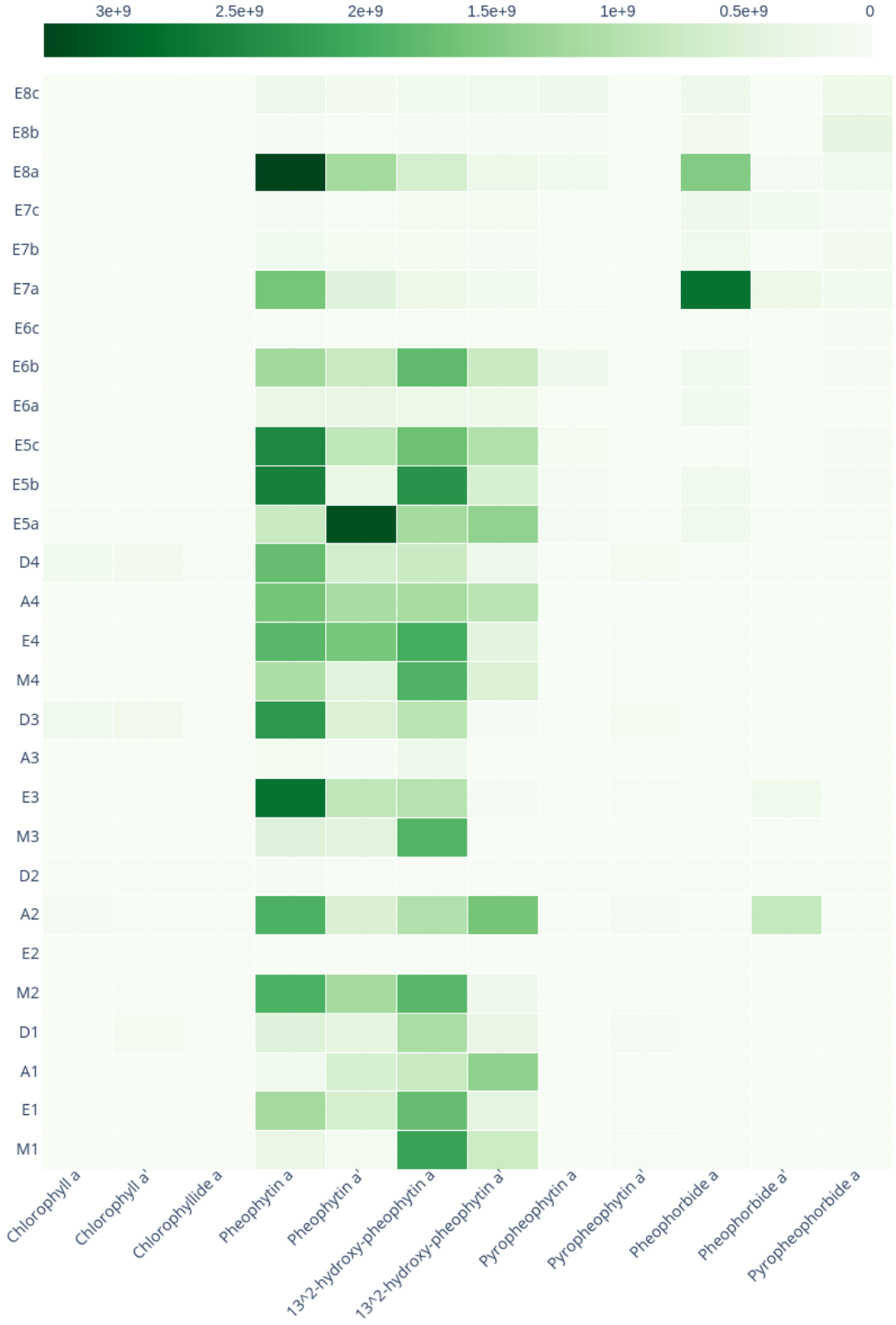

Figure 5 – **Chlorophyll a and its derivatives in crude extracts.** Heatmap resuming the relative abundance of chlorophyll a and its derivatives. The green gradient corresponds to detected peak areas where darker greens represent the higher values while light greens are correlated to lower values.

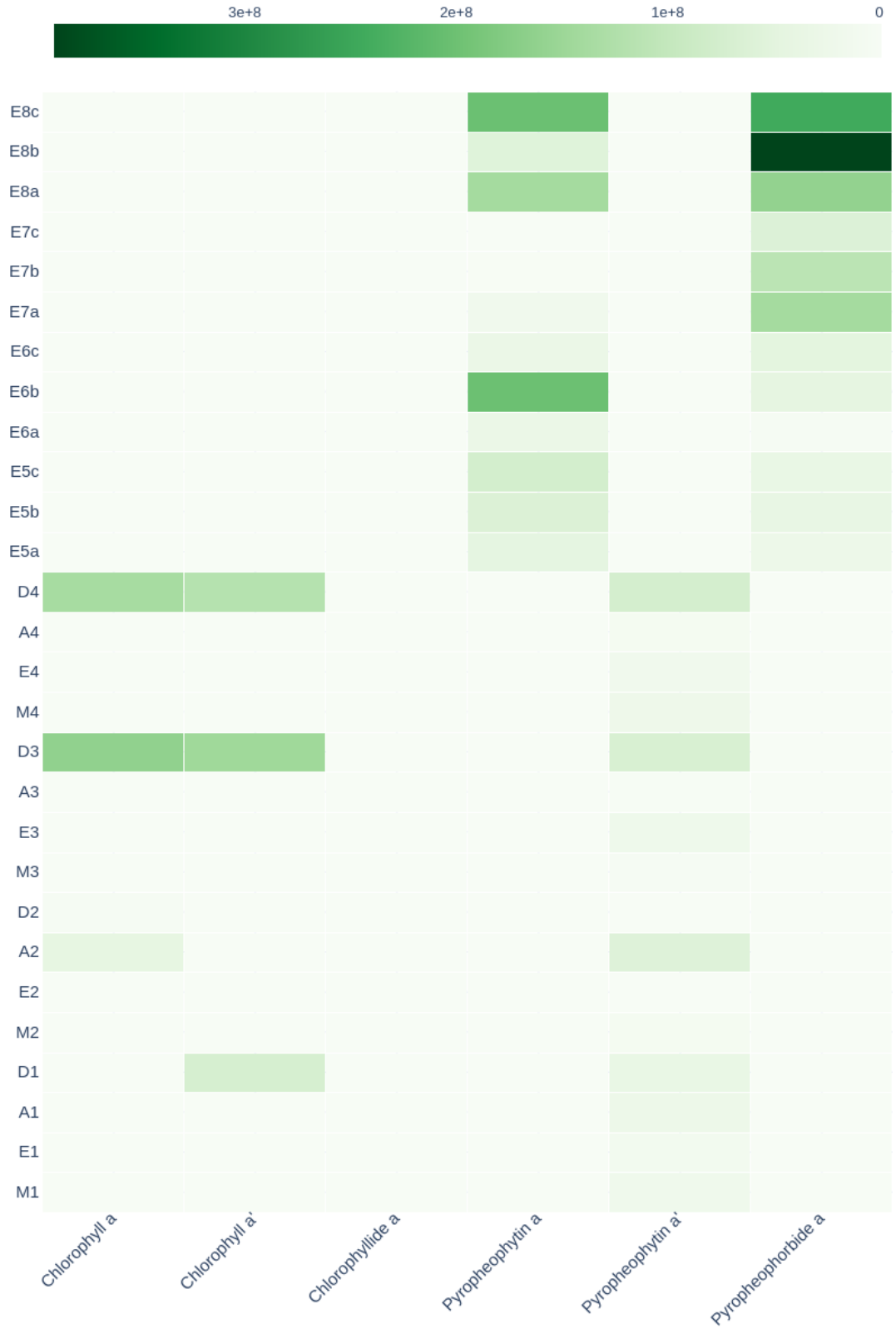

Figure 6 – **Chlorophyll a and its derivatives in crude extracts.** Heatmap resuming the relatively low abundant selected compounds. The green gradient corresponds to detected peak areas where darker greens represent the higher values while light greens are correlated to lower values.

3.3 Bioassays

3.3.1 Zebrafish Nile Red Fat Metabolism Assay

The lipid-reducing potential of each extract was evaluated through the zebrafish Nile Red fat metabolism assay. In the analysis of both prospecting and targeted extractions, REV was employed as a positive control for lipid reduction and DMSO as the solvent control. The fluorescence results were normalised to the DMSO group.

Out of the 16 prospecting extracts, only D1 and E3 demonstrated the capacity to reduce 30-40% of lipid accumulation in zebrafish larvae, as substantiated by the statistically analyses (Figure 7A). Conversely, the results from the targeted extractions presented more promising outcomes, with seven extracts displaying markedly reduced fluorescence, 50-60% less than the solvent control: E5a, E5b, E6a, E6b, E6c, E7c, and E8c (Figure 7B).

In summary, nine extracts exhibited lipid-reduction activity in zebrafish larvae: D1 and E3 from prospecting extractions, and E5a, E5b, E6a, E6b, E6c, E7c, and E8c from targeted extractions.

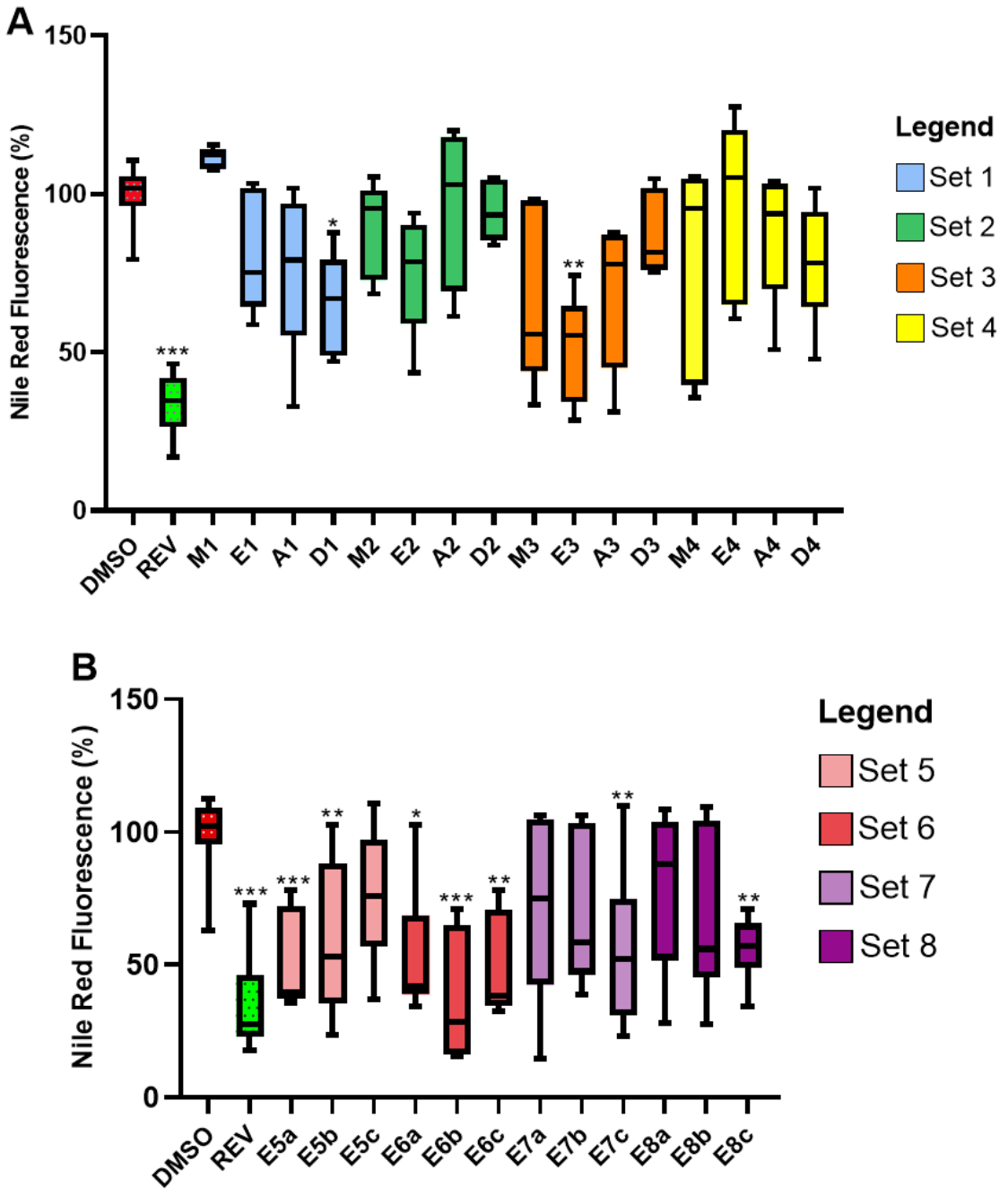

Figure 7 – **Lipid-reducing activity.** Prospecting (A) and targeted (B) extracts data, both diluted in DMSO and at a final concentration of 10 μg/mL in the Nile Red fat metabolism assay using zebrafish larvae. REV at 50 μM was used as positive control for lipid-reducing activity, while DMSO at 0.1% was used as the solvent control. Data are shown relative to DMSO (100%) as box-whisker plots (5-95 percentiles) and were obtained from two independent assays with four individual larvae each (n = 8). Statistically significant different results from DMSO were marked with asterisks (* = $p < 0.05$, ** = $p < 0.01$, *** = $p < 0.001$) on the top of the significant boxes.

3.3.2 Liposome-based Assay for Appetite Reduction

The appetite-reducing activity of each extract was inferred using a liposome-based assay. In the evaluation of both prospecting and targeted extractions, FLX was employed as positive control inhibiting appetite, and a solvent control, DMSO, at 0.1%. The fluorescence results were normalised to solvent control.

Among the 16 prospecting extracts, A1 and A3 were the sole extracts that demonstrated the ability to reduce the appetite of zebrafish larvae at 25% and 50%, respectively, as indicated by the statistical analyses (Figure 7A). In targeted extractions, E5a and E5b, in addition to aforementioned ability to reduce lipid accumulation in zebrafish larvae (Figure 7B), consistently elicited a reduction in appetite in zebrafish larvae at 40% (Figure 8B).

In summary, four extracts exhibited appetite-reduction activity in zebrafish larvae: A1 and A3 from prospecting extractions, and E5a and E5b from targeted extractions.

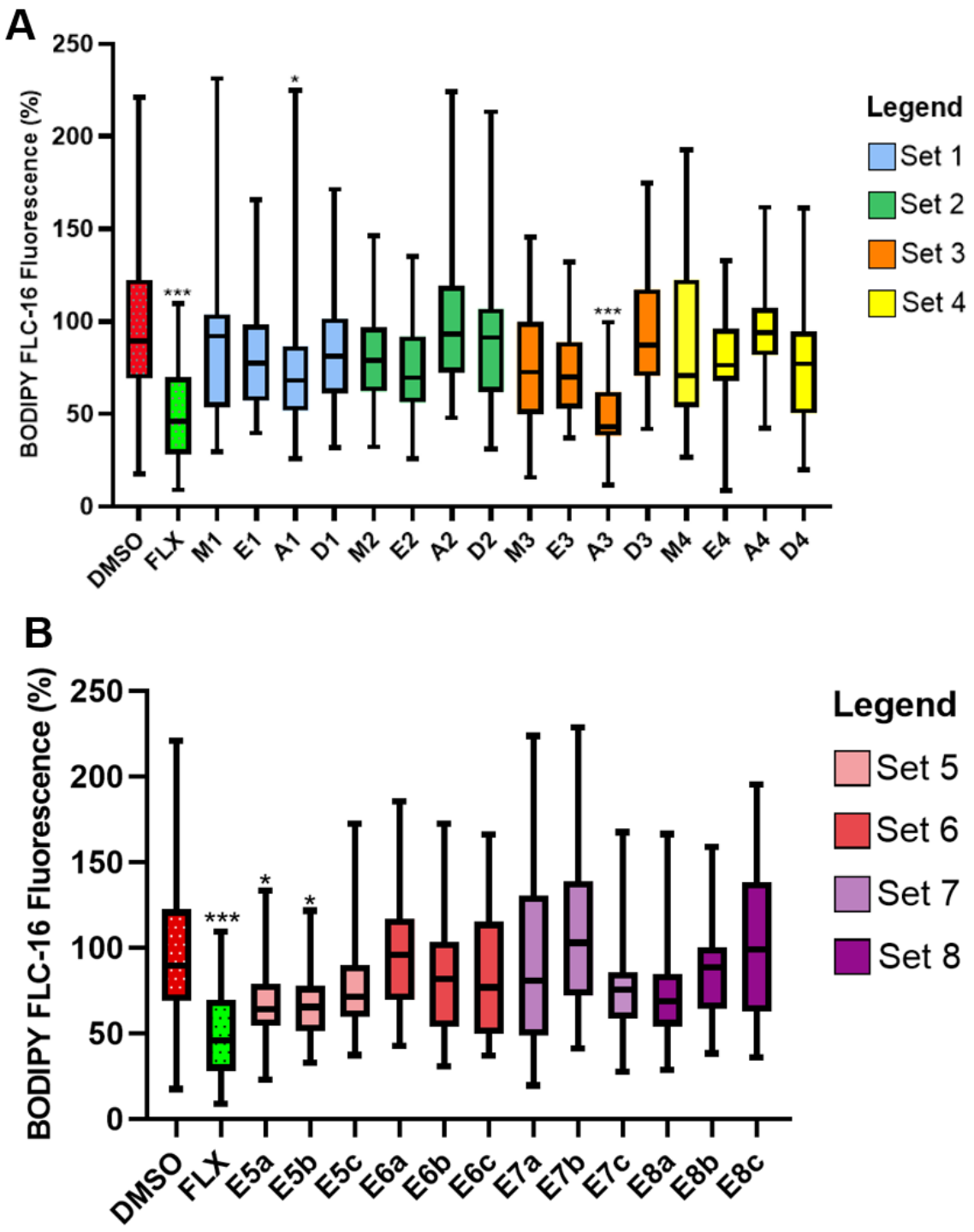

Figure 8 – **Appetite-reducing activity.** Prospecting (A) and targeted (B) extracts data, both diluted in DMSO and at a final concentration of 10 μg/mL in the Liposome-based assay using zebrafish larvae. FLX at 10 mM was used as positive control for appetite-reducing activity, while DMSO at 0.1% was the solvent control. Data are shown relative to DMSO (100%) as box-whisker plots (5-95 percentiles) and were obtained from two independent assays with 6 – 8 individual larvae each (n = 12 – 16). Statistically significant different results from DMSO were marked with asterisks (* = $p < 0.05$, *** = $p < 0.001$) on the top of the significant boxes.

3.4 Putative Bioactive Compounds

3.4.1 Chlorophyll a and its Derivatives and Isomers

The association between the peak area of chlorophyll a derivatives and the extract's bioactivity was established through scatterplots and linear regressions generated using Excel® 2308 Build 16.0.16731.20052. The equations and determination coefficients (R^2) were calculated for each correlation. In graphical representations, peak area values (y-axis) were normalised (Log_{10}), while the x-axis indicates the MFI values, which are linked to the bioactivity of each extract.

For each graph that seeks for the correlation between lipid-reducing activity and peak area of each compound (Figures 9A – 9K), two reference lines were included: one denoting the positive bioactivity control, REV, and another representing the solvent control, DMSO. These lines facilitated the interpretation of bioactivity, with extracts closely aligned with the green line (REV) exhibiting a higher lipid-reducing activity, in contrast to those proximate to the red line (DMSO).

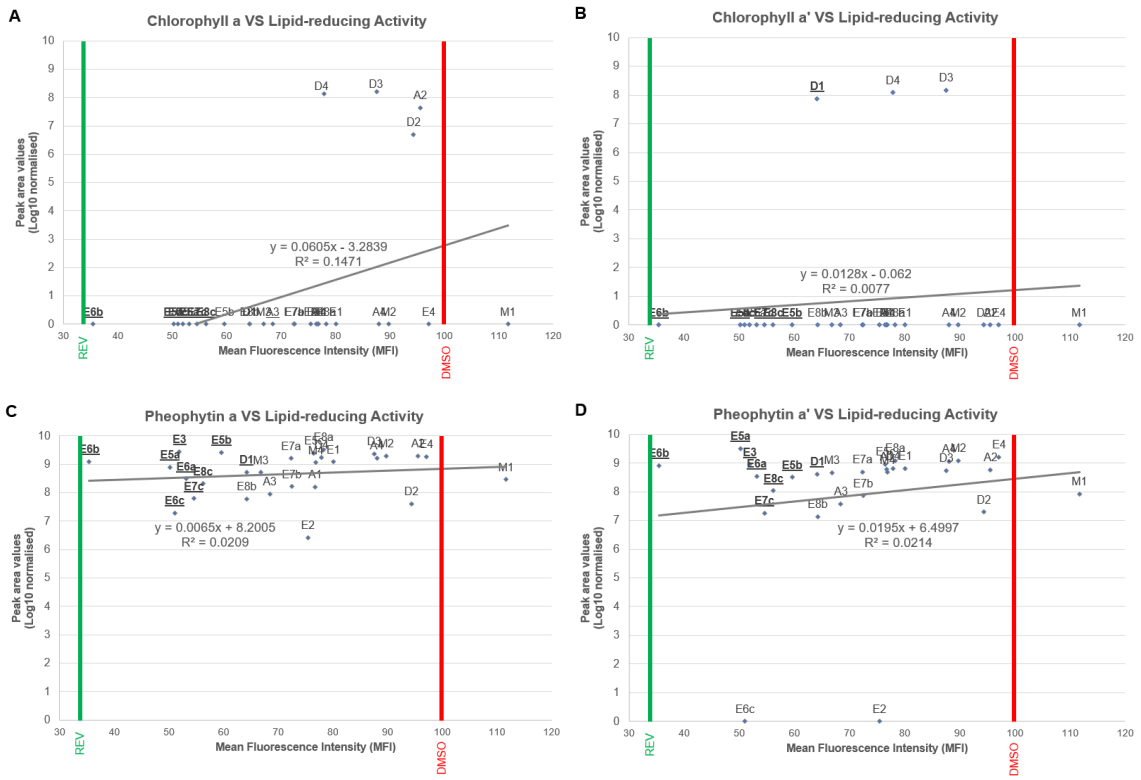

Figure 9 – **Chlorophyll a and its derivatives and isomers vs. lipid-reducing activity.** Peaks area were obtained from raw LC-HR ESI-MS/MS data using Xcalibur 4.1 software. The mean of MFI was calculated after the removal of outliers. All graphs were created in Excel® 2308 Build 16.0.16731.20052, as well as the R^2 calculation and the trend line equation. The control lines – green (REV) and red (DMSO) – were artificially introduced to aid in the interpretation of results.

Figure 9 – Cont.

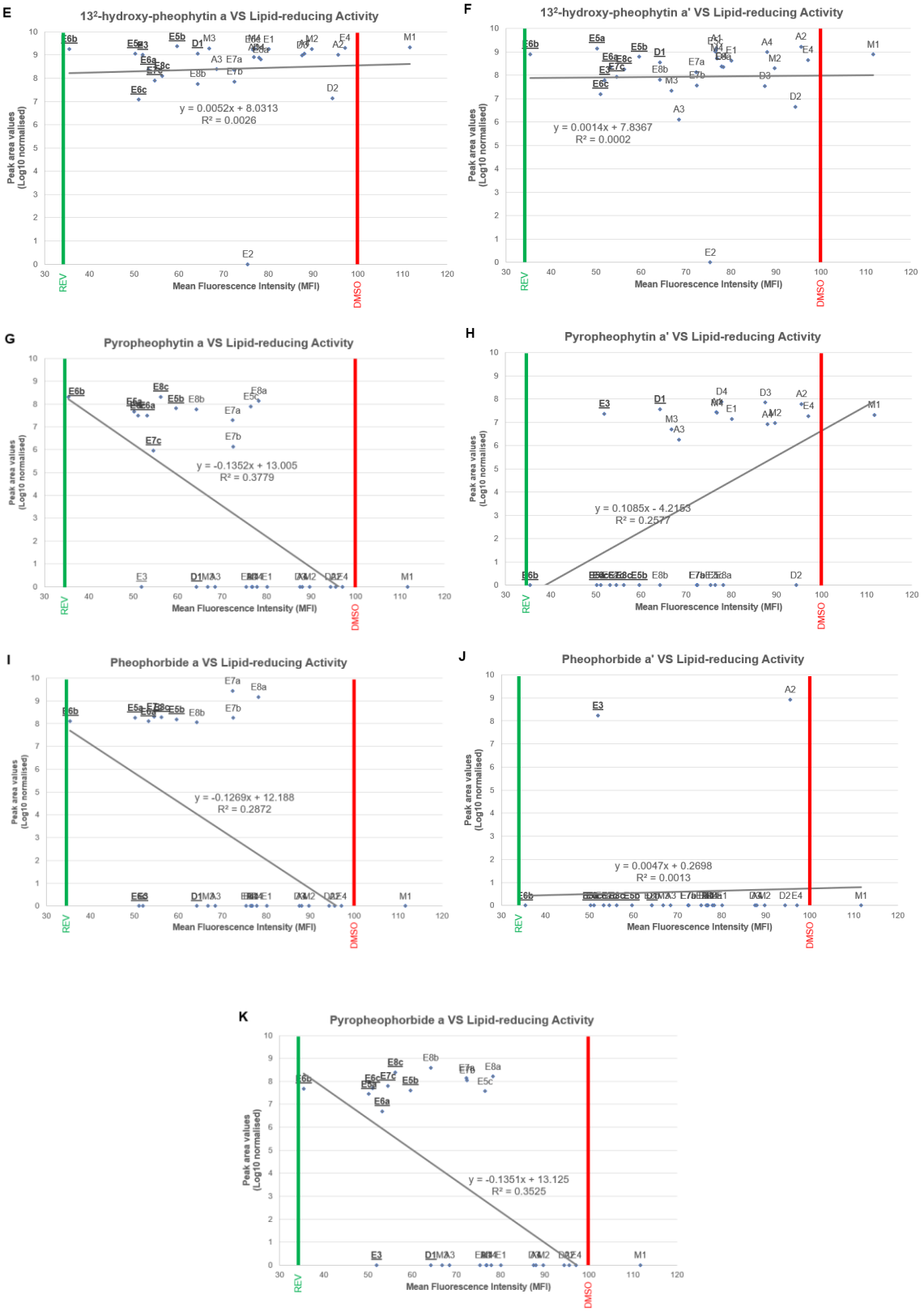

The same principles were applied to the graphs with the appetite-reducing activity (Figures 10A – 10K). However, in this instance, the positive bioactivity control employed was FLX.

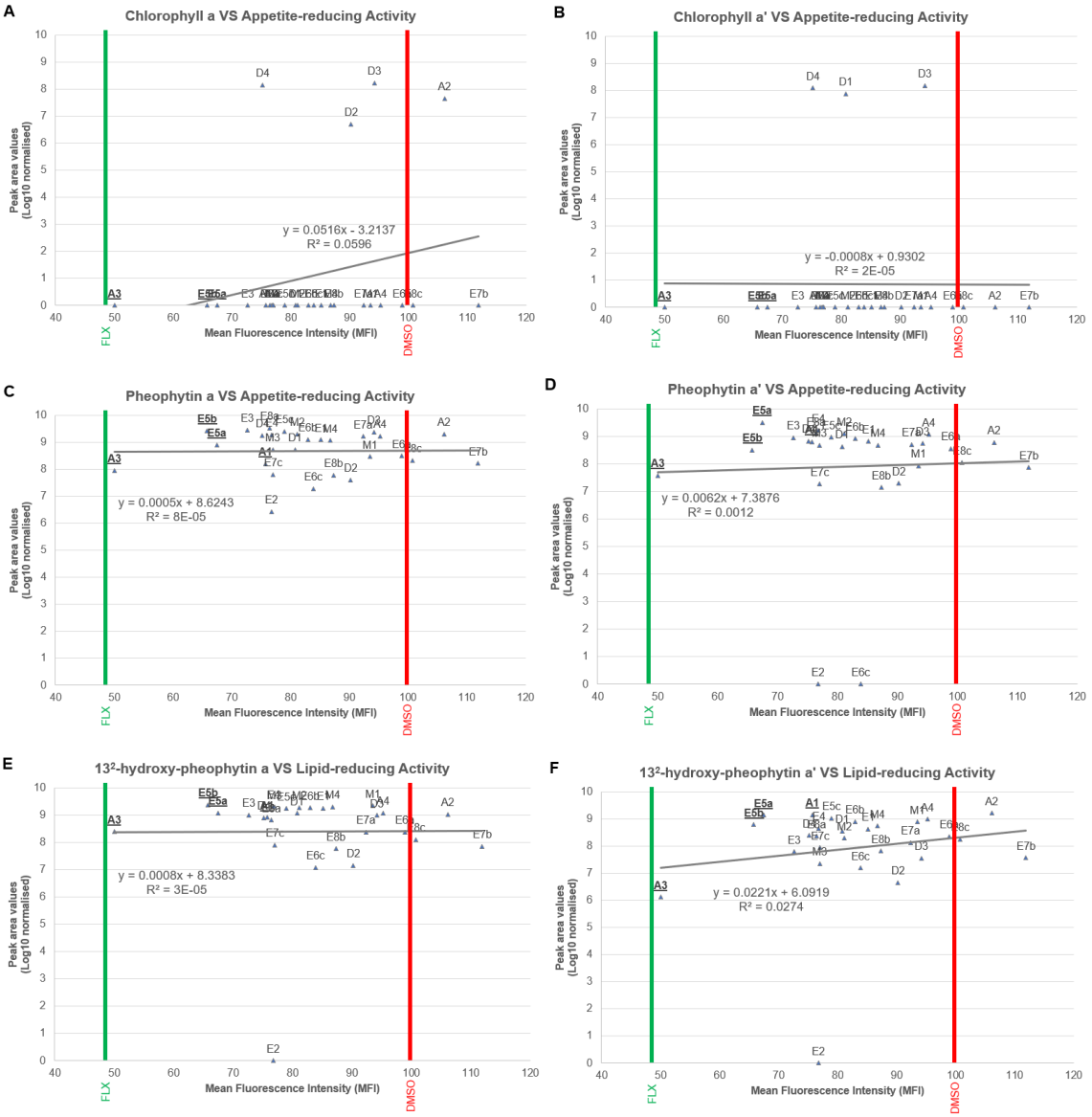

Figure 10 – **Chlorophyll a and its derivatives and isomers vs. appetite-reducing activity.** Peak areas were obtained from raw LC-HR ESI-MS/MS data using Xcalibur 4.1 software. The mean of MFI was calculated after the removal of outliers. All graphs were created in Excel® 2308 Build 16.0.16731.20052, as well as the R^2 calculation and the trend line equation. The control lines – green (FLX) and red (DMSO) – were artificially introduced to aid in the interpretation of results.

Figure 10 – Cont.

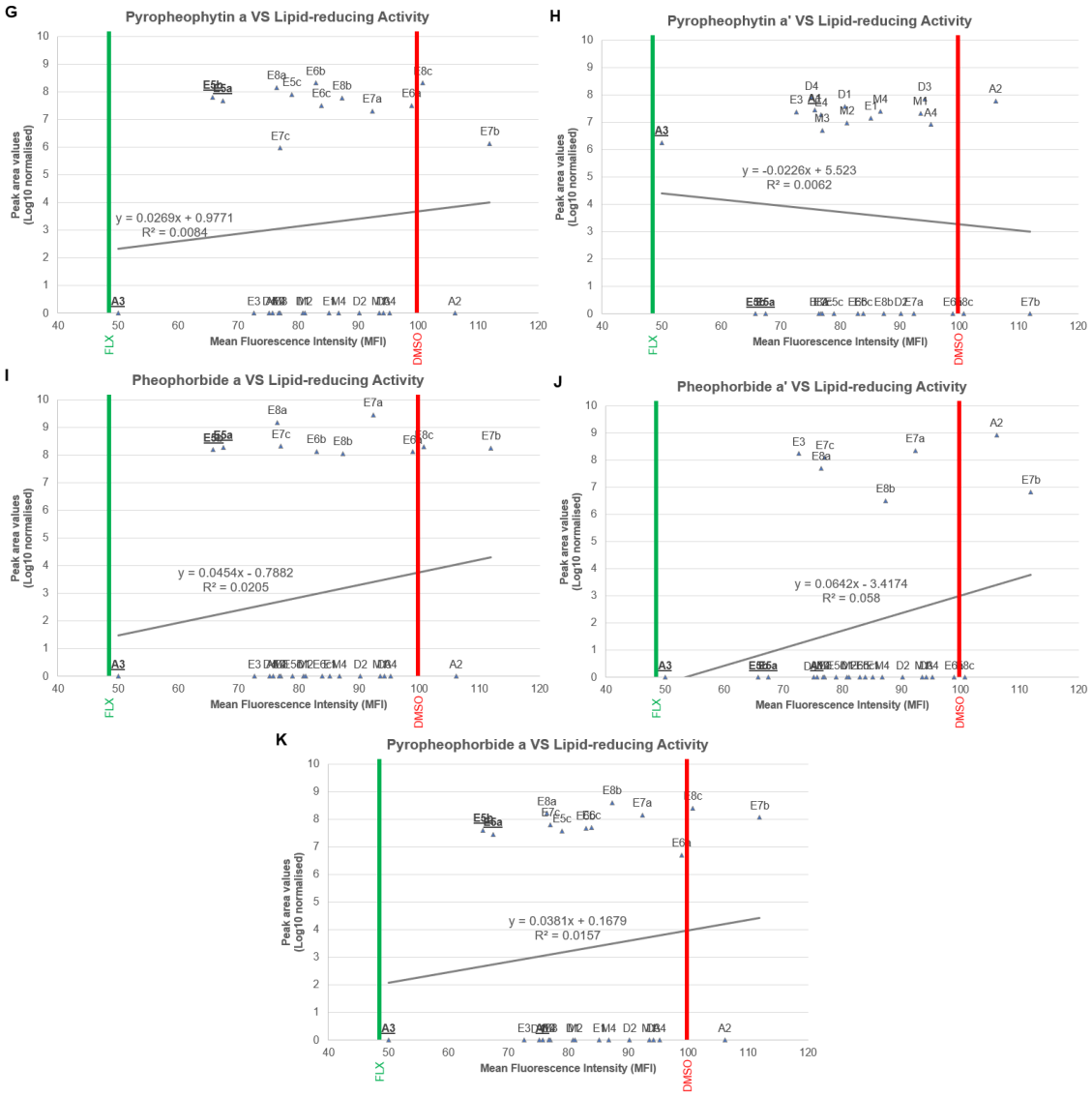

None of the trendlines identified a strong correlation between peaks area of the chlorophyll a derivatives and the observed bioactivities in each assays, as indicated by the low R^2 values.

3.4.2 GNPS Matches

For untargeted metabolite profiling, two molecular networks were constructed: one for prospecting extractions and another for the targeted extractions. Thus, two GNPS MolNetEnhancer workflows incorporated the results of several previous analyses, including NAP, DEREPLICATOR, and MS2LDA, enabling a better identification and annotation of the nodes. These molecular networks were analysed using Cystoscape 3.9.1 software. As a result, the putative identifications of the nodes present in the bioactive extracts provided by the GNPS analysis could be confirmed through their presence in the chromatogram and the calculation of mass errors.

In Figure 11, the metabolic profile of the prospecting extractions is represented. In this molecular network, the compounds present in the extracts of prospective extractions with lipid-reducing activity (D1 and E3) are highlighted. Thus, the larger blue circles represent nodes found only in D1, while the nodes unique to E3 are represented in orange. Additionally, the two nodes shared by both extracts are highlighted in red. None of these nodes were putatively identified by GNPS. However, some unique nodes to E3 were grouped in chlorin cluster, close to some chlorophyll derivatives such as pheophytin a, pyropheophytin a, and pheophorbide a (Figure 12). Besides, a node with 889.582 *m/z* and a retention time of 13.49 mins was noted close to bacteriopheophytin node.

Figure 11 – **Metabolite Profiling of Prospecting Extractions using LC-HR ESI-MS/MS and GNPS.** Unique nodes found exclusively in lipid-reducing bioactive extracts D1 (blue) and E3 (orange) are highlighted in larger sizes. Nodes found in both extracts have a higher size and red colour.

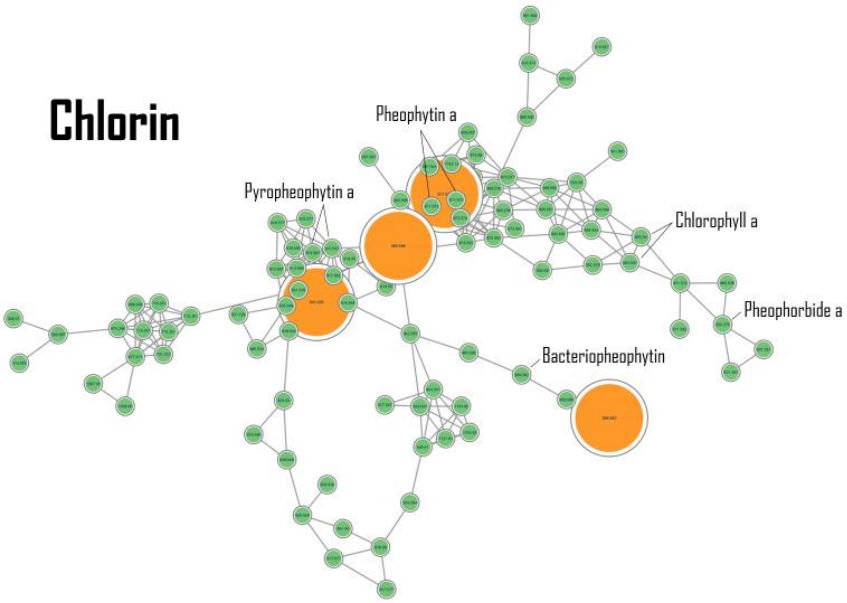

Figure 12 – **Chlorin cluster in Prospecting Extractions.** Four unique nodes found in lipid-reducing bioactive extract E3 (orange) are highlighted in larger sizes. Chlorophyll a and some of its derivatives were also noted in the cluster.

The same analysis was conducted for the remaining activities and extracts (Figures S1 – S3). The resulting data from this analysis are summarised in the Venn diagrams (Figure 13). These diagrams show the number of unique nodes in each extract, as well as those shared among extracts from the same extraction group and with the same activity. Figures 13A to 13D include extracts with lipid-reducing activity, while Figures 13B and 13E include extracts with appetite-reducing activity.

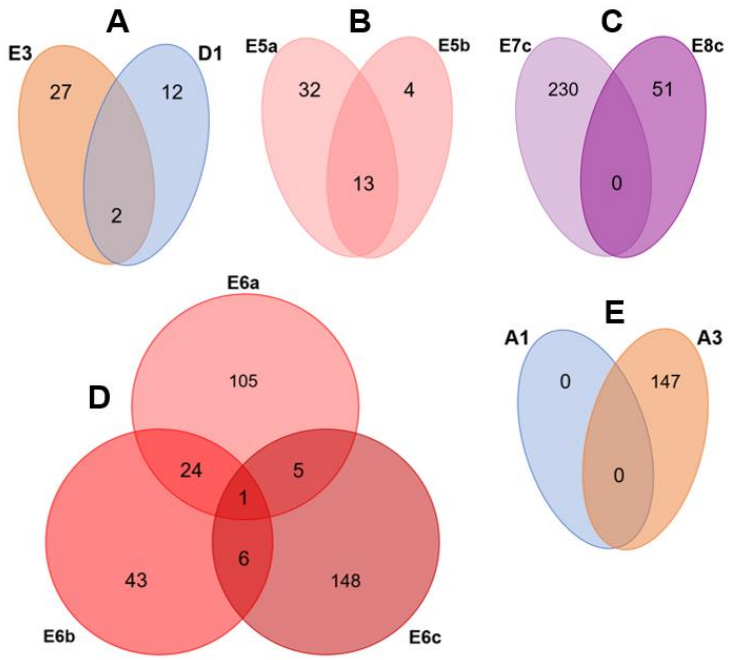

Figure 13 – **Node number in bioactive extracts.** The data were directly collected from the molecular networks. Diagrams A E pertain to the extracts from prospecting extractions with lipid and appetite-reducing activities, respectively. On the other hand, B, C, and D diagrams represent data from the extracts of targeted extractions with lipid-reducing activity. Diagram B also represents the number of nodes in the extracts with appetite-reducing activity.

In total, 850 nodes were identified, however, only 9 of them were putatively identified and listed in Table 5. Thus, the compounds cyclo (Leu-Leu), cyclo (Phe-Leu), 5'-methylthioadenosine, cyclo(L-Leu-L-Pro), guanosine-5'-monophosphate, and cytidine 3'-monophosphate were found in the lipid-reducing activity extracts, while adenosine and ergothioneine were putatively identified in the appetite-reducing activity extracts. In addition to these, D-Tryptophan was identified in extracts with both bioactivities (A3 and E6a).

Table 5 – **Putative Identification of unique compounds in the bioactive extracts.** The identifications were derived from both molecular networks for prospecting and targeted extractions, by GNPS tools. These identifications were based on the MS fragmentation on GNPS and *m/z* values +/− 0.002 against the GNPS database. Possible matches were only considered if the calculated mass error was lower than 5 ppm. $[M+H]^+$: mass + hydrogen mass; Rt: retention time, in minutes; ppm: parts per million.

Sample	$[M+H]^+$	Rt (min)	Putative Identification	Ppm error	Formula
A3	268.104	0.66	Adenosine	1.86	$C_{10}H_{13}N_5O_4$
	230.096	5.48	Ergothioneine	0	$C_9H_{15}N_3O_2S$
	205.097	0.78	D-Tryptophan	0	$C_{11}H_{12}N_2O_2$
E6a		0.71			
E6c	227.175	4.83	Cyclo(Leu-Leu)	4.40	$C_{12}H_{22}N_2O_2$
	261.159	5.14	Cyclo(Phe-Leu)	1.34	$C_{15}H_{20}N_2O_2$
E6a ∩ E6b	298.097	0.65	5'-Methylthioadenosine	0	$C_{11}H_{15}N_5O_3S$
E6a ∩ E6b ∩ E6c	211.144	2.35	Cyclo(L-Leu-L-Pro)	0	$C_{11}H_{18}N_2O_2$
E8c	364.065	0.66	Guanosine-5'-monophosphate	0	$C_{10}H_{14}N_5O_8P$
	324.059	0.58	Cytidine 3'-monophosphate	0	$C_9H_{14}N_3O_8P$

4. Discussion

The extraction of chlorophylls and their derivatives from *A. platensis* biomass can be carried out using two types of extraction methodologies: (i) non-mechanical methods, such as chemical, thermal, or enzymatic, and/or (ii) mechanical methods, such as pressurised systems, sonication, microwave, electric fields, and supercritical extractions. It is common to combine these methodologies (92,93). Classic extraction methods often utilise both methodologies, combining solvents and thermal treatments (heat or cold) associated with sonication to promote cell disruption (92,93). In addition to these methods, supercritical fluid extraction has gained prominence as the most effective and clean method for extracting pigments like carotenoids and chlorophylls, using carbon dioxide as a solvent. However, the main limitation of this methodology remains the high implementation and operational costs, unlike classic methods. Thus, classic methodologies remain relevant for obtaining enriched extracts in chlorophylls and their derivatives, and this strategy was implemented in the extractions performed in this work.

Initially, four sets of extractions were established: 1, 2, 3, and 4, which differed in conditions to evaluate the effect of the solvent used (methanol, ethanol, acetone, and dichloromethane), cell disruption, heating during extraction, and post-acidification of the extracts. The quantity and colour of the extracts were annotated as well as the relative abundance of chlorophyll a and its expected derivatives. Thus, 16 extracts were obtained (M1, E1, A1, D1, M2, E2, A2, D2, M3, E3, A3, D3, M4, E4, A4, and D4) and analysed using the LC-HR ESI-MS/MS technique. The relative abundance of the selected compounds was inferred by detecting peak areas in the chromatograms.

Higher peak areas of chlorophyll a were detected in extracts obtained from extractions where dichloromethane was used, particularly in D3 and D4. This apparent enhanced extraction of chlorophyll a can be explained by the nature of this molecule. Chlorophyll a is poorly soluble in water and soluble in organic solvents, as utilised in each of the prospecting extractions sets (sets 1, 2, 3, and 4). In chloroplasts, chlorophylls are bound to nonpolar compounds such as carotenoids, lipids, and lipoproteins through noncovalent bonds (71). This results in extractions with more nonpolar solvents yielding dark green extracts enriched in chlorophyll a. Therefore, it is consistent that the higher relative abundance of this pigment was detected in extracts resulting from extractions where dichloromethane, the most nonpolar of the tested solvents, was employed. However, extractions using this solvent produced smaller quantities of crude extract (Figures 4C and 4D) and proved to be less effective in

extracting the other analysed compounds (Figure 5). Additionally, dichloromethane is a solvent that tends to be avoided due to its toxicity (94).

Considering the disadvantages of using dichloromethane, in previous studies, safer solvents like ethanol have proven to be viable for the extraction of chlorophyll a. In a study of optimisation of chlorophyll a extraction processes published in 2017 by Choi *et al*., ethanol/H_2O (7/3, v/v) was used as a solvent in an optimal ultrasonication extraction at 32.59 ºC for 4.91 hours, yielding 17.98 mg/g of chlorophyll a from 100 g of spirulina (95). Besides the effectiveness of using ethanol for chlorophyll a extraction, this study also emphasised the importance of sonication for efficient extraction. This conclusion is consistent with our results, as extracts subjected to ultrasonic frequencies (all sets except set 2) showed a higher relative abundance of chlorophyll a and its derivatives, compared to set 2 where sonication was not performed.

Regarding the extraction of the selected derivatives, the pheophytins (pheophytin a, pheophytin a', 13^2-hydroxy-pheophytin a, and 13^2-hydroxy-pheophytin a') were the analysed derivatives with the highest peak areas, while the pyro-derivatives (pyropheophytin a and pyropheophorbide) were mostly detected in the extreme conditions (targeted extractions) and showed low peak areas. Chlorophyllide a was not detected in any performed extraction, however, previous studies showing that it is possible to obtain extracts enriched in this compound from barley leaves (*Hordeum vulgare* L.) ground them in liquid nitrogen and then suspended in 80% acetone (acetone/50 mM Tricine–NaOH, pH 8, 80:20, v/v). The suspension was repeatedly extracted with hexane, added to diethyl ether/ethanol (1:1), and then repeatedly washed with 100 mL of 20% EtOH (10 mM Tricine-NaOH, pH 8) (96). The milking *Rhodobacter capsulatus* CB1200 cultivated in a medium containing Tween 80 was also considered an efficient methodology to obtain chlorophyllide a (96). Low peak areas of pheophorbides were found for most of the extractions, however, the isomer pheophorbide a' was detected in extract A2, besides the lack of the sonication step.

Overall, these results indicated a relatively low degradation of chlorophyll a in these initial extractions. Consequently, a new set of extractions was designed and carried out – targeted extractions. In this new group, harsh conditions such as extraction temperature and post-acidification of the extracts were intentionally intensified to obtain more degraded derivatives of chlorophyll a, such as pyro-derivatives. The extraction time was extended, while the solvent (ethanol 70%), sonication step, and dark extraction conditions remained consistent across all targeted extractions. In this new group, higher peak areas of pheophorbide a were detected,

especially for the 1-hour extractions with post-acidification, with a temperature of 80 ºC (E7a) proving more effective than 100 ºC (E8a) (Figure 5). For chlorophyll a and chlorophyllide a, no peaks were detected as expected given the extraction conditions applied. In the study of Che *et al*., it was demonstrated that it is possible to obtain pheophytin a through acidification with HCl (0.04 N HCl in isopropanol) of a solution of isolated chlorophyll a dissolved in diethyl ether (95). From the same solution, it was also possible to obtain 13^2-hydroxy-pheophytin a by applying a treatment at 70 ºC for 3 hours (97). The same research group was also able to produce pyro-derivatives (pyropheophytin a and pyropheophorbide a) after treatment at 80 ºC for 4 hours of the previously described solution (97,98). Therefore, the relative increase in the detection of pyro-derivatives in the targeted extractions is consistent with the existing literature.

After the relative quantification of chlorophyll a and its derivatives, each one of the 28 extracts was tested to evaluate their lipid-reducing and appetite-reducing activities, both tested in zebrafish larvae. The use of these organisms as a model has gained popularity due to their high physiological and genetic similarity with mammals, low-cost maintenance, and rapid development. Additionally, several similarities in lipid metabolism between these organisms and mammals have been described (99). The zebrafish Nile Red fat metabolism assay enabled the measurement of neutral lipid content (in the intestine and yolk sac region) in zebrafish larvae, allowing us to determine if certain compounds have lipid-reducing activity (99). This assay has been successfully employed in previous studies for screening new secondary metabolites from cyanobacterial fractions or in studies focused on isolating known and novel chlorophyll a derivatives, such as 13^2-hydroxy-pheophytin a and 13^2-hydroxy-pheofarnesin a, from the cyanobacteria *Nodosilinea* sp. and *Cyanobium* sp. (50,100). On the other hand, the liposome-based assay is a protocol used to test the influence of extracts or pure compounds on the appetite of zebrafish larvae, comparing their action with the previously well-described appetite-reducing compound fluoxetine (81).

As a result, nine extracts (D1, E3, E5a, E5b, E6a, E6b, E6c, E7c, and E8c) exhibited lipid-reducing activity, while four extracts (A1, A3, E5a, and E5b) were capable of reducing the appetite of zebrafish larvae. When investigating a possible linear relationship between the peak area of the analysed compounds and the bioactivity of the extracts (as indicated by the MFI values), it was concluded that it was not possible to establish any such relationship between the data. Nevertheless, in the aforementioned investigation of Freitas *et al.*, 13^2-hydroxy-pheophytin a at a concentration of 10 µg/mL showed promising lipid-reducing activity in zebrafish larvae (50), suggesting that an optimal concentration of this compound may be necessary for

lipid reduction, or the interaction with other compounds present in the crude extracts may have hindered the effects previously reported. For this reason, the fractionation of these bioactive extracts will aid in understanding which compounds are responsible for the bioactivity. In addition, other studies have also reported the benefits of spirulina biomass consumption and the action of extracts for both bioactivities tested in this work. In a review article published in 2020 by DiNicolantonio *et al*., several pieces of evidence were compiled regarding the benefits the supplementation with spirulina biomass, in both zebrafish and mice model organisms, and even in clinical trials performed in humans. These benefits included anti-inflammatory properties, assistance in weight loss due to the ability to inhibit pancreatic lipases and improved satiety. Additionally, it has shown the ability to regulate cholesterol levels by promoting its excretion and improving dyslipidaemia (69).

In parallel, the untargeted metabolomic analysis allowed the analyses of the metabolic profiles of both extraction groups and the annotation of unique and shared nodes among the bioactive extracts. As a result, 850 nodes were annotated, 51 of which were present in two or more bioactive extracts. Nine nodes were putatively identified, six of them (cyclo(Leu-Leu), cyclo(Phe-Leu), 5'-methylthioadenosine, cyclo(L-Leu-L-Pro), guanosine-5'-monophosphate, and cytidine 3'-monophosphate) were detected in extracts with lipid-reducing activity, while other 2 (adenosine and ergothioneine) were detected in extracts capable of reducing the appetite of zebrafish larvae. Additionally, a node putatively identified as D-tryptophan was found in extracts with both bioactivities.

Both cyclo(Leu-Leu) and cyclo(Phe-Leu) are cyclic dipeptides. The cyclo(Leu-Leu) has shown properties of being anti-biofilm and anti-adherent against the cariogenic bacterium *Streptococcus mutans* and the pathogenic fungus *Candida albicans* (101). However, studies about the cyclo(Phe-Leu) properties are lacking. Cyclic(L-Leu-L-Pro) was described to inhibit the migration of breast cancer cells, beyond its well-recognised antimicrobial and antioxidant activities (102). No described activities for reduction of lipids or suppression of appetite were found in the scientific literature.

5'-Methylthioadenosine (MTA) is a byproduct of S-adenosylmethionine (SAM) catabolism, and it plays a fundamental role in the methylation of numerous molecules. Previous studies have demonstrated that a diet rich in methyl group donors prevented the progression of NAFLD in mice, primarily by enhancing hepatic beta-oxidation of

lipids (103). Nevertheless, direct investigations into the impact of MTA on appetite regulation remain imperative.

Guanosine-5'-monophosphate (5'-GMP), cytidine 3'-monophosphate (3'-CMP), and adenosine are important nucleotide molecules for the synthesis of nucleic acids such as DNA and RNA. Furthermore, 5'-GMP has been shown to evoke the umami taste sensation (104), making it potentially useful in the development of dietary products. 3'-CMP is an intermediate in the nucleotide cytidine. These compounds have demonstrated to alleviate certain aspects of dyslipidaemia and to improve hepatic steatosis by modulating the gut microbiota composition in mice (105). The putative presence of adenosine in the extracts capable of reducing appetite is intriguing. In a study on the molecular implications of this molecule in obesity, published in 2017 by Pardo *et al*., no direct relationship was established between this compound and appetite (106). However, a prior study published by Levine *et al.,* in 1983, reported a suppression of appetite of rats after a 50 mg/kg dose intracerebroventricular injected (107), although further research is required to explore this relationship.

Ergothioneine (EGT) is a potent dietary antioxidant amino acid, first discovered in 1909 in the ergot fungus (*Claviceps purpurea*) (108,109). Dietary supplementation with EGT-rich mushrooms proved to be beneficial to diabetics (110) and could reduce systemic oxidative stress and inflammatory markers (111).

Lastly, the putatively detected D-tryptophan in extracts exhibiting both activities is an essential amino acid capable of inducing satiety in humans (112). More recently, dietary supplementation with tryptophan reduced the hepatic lipogenesis and gluconeogenesis in piglets (113), however, further research will be necessary to test the direct effect of D-tryptophan on lipid reduction and appetite suppression.

The putative identification of these compounds in spirulina extracts is an encouragement to continue studying the potential of its metabolites, reinforcing the significant contribution of powerful metabolomic analysis tools in the field of research on compounds with pharmaceutical, nutraceutical, or industrial potential, whether they are derived from chlorophyll or not.

5. Conclusion

The ongoing global obesity epidemic exerts a profound and far-reaching impact on quality of life while presenting a significant challenge to public health. Despite the implementation of numerous solutions and strategies, their effectiveness remains limited. Pharmaceuticals often come with adverse side effects, with only a handful considered safe by regulatory authorities. This realisation has spurred both scientists and the industry to explore the untapped potential of natural products as innovative remedies. Notably, derivatives of chlorophyll a have recently emerged as promising candidates in the fight against obesity. These pigments could be found among several sources like the relatively unexplored cyanobacteria. This phylum holds a treasure trove of these and other metabolites, offering immense potential for various human applications. Particularly, the *Arthrospira* genus has garnered substantial attention, being approved for human food consumption.

In the context of our research, *A. platensis* was chosen as a source of chlorophyll a and its derivatives due to its high amounts of this pigment. Also, this cyanobacterium has already been associated with a range of bioactivities, including its ability to reduce lipid levels. Following recent discoveries of two hydroxy-pheophytins with lipid-reducing activity, twenty-eight extraction procedures were conducted to optimise the extraction of chlorophyll a derivatives. Additionally, the lipid and appetite-reducing activities of each obtained extract were analysed. These extracts were also subjected to an in-depth analysis using LC-HR ESI-MS/MS.

The present findings revealed that the extraction conditions had a discernible impact on the yield of chlorophyll a and its derivatives. According to MS data, dichloromethane emerged as the most effective solvent for chlorophyll a extraction, despite its inherent toxicity. Additionally, our research demonstrated that ethanolic extractions conducted at temperatures equal to or exceeding 80°C yielded extracts enriched in pheophytins, including the lipid-reducer 13^2-hydroxy-pheophytin a, after 1-2 hours of extraction. By introducing an additional post-treatment with HCl, a higher relative abundance of pheophorbide a was detected. It is important to note that the current study could not provide detailed extraction protocols for pyro-derivatives such as pyropheophytin a or pyropheophorbide a. Nevertheless, a clear association between high temperatures with post acidification and the synthesis of pyropheophorbide a was observed.

These efforts culminated in the acquisition of 9 bioactive extracts that merit further exploration through fractionation and the quest for bioactive compounds. The putative identifications outlined in this study could offer valuable insights into the origins of the bioactivity present in these extracts. Noteworthy, some of the identified compounds had described lipid reducing or appetite reducing activities from the scientific literature.

In conclusion, spirulina represents a rich source of chlorophyll a and its derivatives, with its extracts holding significant potential in the ongoing battle against obesity. The in-depth investigation of the composition of these extracts may pave the way for the development of safer and more effective novel treatments for obesity, making a substantial contribution to the global endeavour to combat this pressing public health challenge.

6. Future Work

While this study has successfully established effective protocols for the extraction of pheophytins, none of the tested procedures demonstrated efficacy in the extraction of pyro-derivatives from spirulina biomass. Subsequent investigations may seek to build upon the successful extraction protocols for pheophytins here elucidated, and expose them to degradative conditions, such as prolonged exposure to high temperatures, as a potential strategy to produce pyro-derivatives, for instance.

Regarding the bioactive extracts obtained, the next research phase may involve a bioassay-guided isolation strategy, aiming at the purification of bioactive compounds. This process will entail a meticulous assessment of their suitability as novel anti-obesity nutraceuticals. Thus, each bioactive extract should undergo sequential fractionation steps, utilising techniques such as Vacuum Liquid Chromatography and High-Performance Liquid Chromatography. The lipid and appetite-reducing activities can be assessed using the methodology described in the present work.

To enhance the understanding of these bioactive fractions, the putatively identified compounds could be acquired commercially and tested for their bioactivities as individual compounds in a range of concentrations. Additionally, non-active extracts and fractions could be subjected to assessments for other potential activities, including antioxidant or anti-adherent properties, amongst others, which could result in an expanding of their applicabilities, avoiding waste these crude extracts.

An equally crucial aspect of the future work revolves around the elucidation of the mechanisms of action of the bioactive compounds that may be discovered. It is also essential to explore their safety profiles before advancing into human clinical trials. Finally, the efficacy of these bioactive compounds must be compared with existing options to assess their potential relevance within the pharmaceutical and nutraceutical markets.

7. References

1. Wu J, Boström P, Sparks LM, Ye L, Choi JH, Giang A-H, et al. Beige adipocytes are a distinct type of thermogenic fat cell in mouse and human. Cell. 2012 Jul 20;150(2):366–76.
2. Castro M, Preto M, Vasconcelos V, Urbatzka R. Obesity: The Metabolic Disease, Advances on Drug Discovery and Natural Product Research. Curr Top Med Chem. 2016 Jul 1;16(23):2577–604.
3. Lin X, Li H. Obesity: Epidemiology, Pathophysiology, and Therapeutics. Front Endocrinol (Lausanne). 2021 Sep 6;12(September):1–9.
4. WHO. Obesity and overweight [Internet]. 2021 [cited 2022 Dec 10]. Available from: https://www.who.int/news-room/fact-sheets/detail/obesity-and-overweight
5. Chooi YC, Ding C, Magkos F. The epidemiology of obesity. Metabolism. 2019 Mar;92:6–10.
6. Aronne LJ, Nelinson DS, Lillo JL. Obesity as a disease state: a new paradigm for diagnosis and treatment. Clin Cornerstone. 2009;9(4):9–29.
7. Wright SM, Aronne LJ. Causes of obesity. Abdom Imaging. 2012 Oct;37(5):730–2.
8. Swinburn BA, Sacks G, Hall KD, McPherson K, Finegood DT, Moodie ML, et al. The global obesity pandemic: shaped by global drivers and local environments. Lancet. 2011 Aug;378(9793):804–14.
9. Penzias A, Azziz R, Bendikson K, Falcone T, Hansen K, Hill M, et al. Obesity and reproduction: a committee opinion. Fertil Steril. 2021 Nov 1;116(5):1266–85.
10. EASO. Statistics - EASO [Internet]. 2023. Available from: https://easo.org/media-portal/statistics/
11. Oliveira A, Araújo J, Severo M, Correia D, Ramos E, Torres D, et al. Prevalence of general and abdominal obesity in Portugal: Comprehensive results from the National Food, nutrition and physical activity survey 2015-2016. BMC Public Health. 2018 May 11;18(1):1–9.
12. Páscoa R, Teixeira A, Henriques TS, Monteiro H, Monteiro R, Martins C. Characterization of an obese population: a retrospective longitudinal study from real-world data in northern Portugal. BMC Prim Care. 2023 Dec 1;24(1):1–12.
13. Okunogbe A, Nugent R, Spencer G, Powis J, Ralston J, Wilding J. Economic impacts of overweight and obesity: current and future estimates for 161 countries. BMJ Glob Heal. 2022 Sep 20;7(9):e009773.
14. Ottaviani E, Malagoli D, Franceschi C. The evolution of the adipose tissue: a neglected enigma. Gen Comp Endocrinol. 2011 Oct 1;174(1):1–4.

15. Koenen M, Hill MA, Cohen P, Sowers JR. Obesity, Adipose Tissue and Vascular Dysfunction. Circ Res. 2021 Apr 2;128(7):951–68.
16. Ramakrishnan VM, Boyd NL. The Adipose Stromal Vascular Fraction as a Complex Cellular Source for Tissue Engineering Applications. Tissue Eng Part B Rev. 2018 Aug;24(4):289–99.
17. Kershaw EE, Flier JS. Adipose Tissue as an Endocrine Organ. J Clin Endocrinol Metab. 2004 Jun;89(6):2548–56.
18. Frigolet ME, Gutiérrez-Aguilar R. The colors of adipose tissue. Gac Med Mex. 2020;156(2):142–9.
19. Cheng L, Wang J, Dai H, Duan Y, An Y, Shi L, et al. Brown and beige adipose tissue: a novel therapeutic strategy for obesity and type 2 diabetes mellitus. Adipocyte. 2021;10(1):48–65.
20. Kawai T, Autieri M V., Scalia R. Adipose tissue inflammation and metabolic dysfunction in obesity. Am J Physiol Cell Physiol. 2021 Mar 1;320(3):C375–91.
21. Saunders KH, Umashanker D, Igel LI, Kumar RB, Aronne LJ. Obesity Pharmacotherapy. Med Clin North Am. 2018;102(1):135–48.
22. Wang F-G, Yan W-M, Yan M, Song M-M. Outcomes of Mini vs Roux-en-Y gastric bypass: A meta-analysis and systematic review. Int J Surg. 2018;56:7–14.
23. Green N. Bariatric surgery: an overview. Nurs Stand. 2012;26(36):48-56: quiz 58, 60.
24. Kang JG, Park C-Y. Anti-Obesity Drugs: A Review about Their Effects and Safety. Diabetes Metab J. 2012;36(1):13–25.
25. Son JW, Kim S. Comprehensive Review of Current and Upcoming Anti-Obesity Drugs. Diabetes Metab J. 2020 Dec 31;44(6):802–18.
26. Gettman L. New Drug: Tirzepatide (Mounjaro ™). Sr Care Pharm. 2023;38(2):50–62.
27. WEIBEL EK, HADVARY P, HOCHULI E, KUPFER E, LENGSFELD H. Lipstatin, an inhibitor of pancreatic lipase, produced by Streptomyces toxytricini. I. Producing organism, fermentation, isolation and biological activity. J Antibiot (Tokyo). 1987;40(8):1081–5.
28. Heck AM, Yanovski JA, Calis KA. Orlistat, a new lipase inhibitor for the management of obesity. Pharmacotherapy. 2000;20(3):270–9.
29. Khera R, Murad MH, Chandar AK, Dulai PS, Wang Z, Prokop LJ, et al. Association of Pharmacological Treatments for Obesity With Weight Loss and Adverse Events: A Systematic Review and Meta-analysis. JAMA. 2016;315(22):2424–34.

30. Shin JH, Gadde KM. Clinical utility of phentermine/topiramate (Qsymia™) combination for the treatment of obesity. Diabetes Metab Syndr Obes. 2013;6:131–9.
31. Jastreboff AM, Aronne LJ, Ahmad NN, Wharton S, Connery L, Alves B, et al. Tirzepatide Once Weekly for the Treatment of Obesity. N Engl J Med. 2022;387(3):205–16.
32. Seo Y-G. Side Effects Associated with Liraglutide Treatment for Obesity as Well as Diabetes. J Obes Metab Syndr. 2021;30(1):12–9.
33. Balaji M, Ganjayi MS, Hanuma Kumar GEN, Parim BN, Mopuri R, Dasari S. A review on possible therapeutic targets to contain obesity: The role of phytochemicals. Obes Res Clin Pract. 2016;10(4):363–80.
34. Yun JW. Possible anti-obesity therapeutics from nature--a review. Phytochemistry. 2010;71(14–15):1625–41.
35. Thomford N, Senthebane D, Rowe A, Munro D, Seele P, Maroyi A, et al. Natural Products for Drug Discovery in the 21st Century: Innovations for Novel Drug Discovery. Int J Mol Sci. 2018;19(6):1578.
36. Hu X, Tao N, Wang X, Xiao J, Wang M. Marine-derived bioactive compounds with anti-obesity effect: A review. J Funct Foods. 2016;21:372–87.
37. Vermaak I, Viljoen AM, Hamman JH. Natural products in anti-obesity therapy. Nat Prod Rep. 2011;28(9):1493.
38. Ligon BL. Penicillin: its discovery and early development. Semin Pediatr Infect Dis. 2004 Jan;15(1):52–7.
39. Molina-Venegas R, Rodríguez MÁ, Pardo-de-Santayana M, Mabberley DJ. A global database of plant services for humankind. Paniagua-Zambrana NY, editor. PLoS One. 2021 Jun 15;16(6):e0253069.
40. Yun B-W, Yan Z, Amir R, Hong S, Jin Y-W, Lee E-K, et al. Plant natural products: history, limitations and the potential of cambial meristematic cells. Biotechnol Genet Eng Rev. 2012 Jan;28(1):47–60.
41. Benyhe S. Morphine: New aspects in the study of an ancient compound. Vol. 55, Life Sciences. Pergamon; 1994. p. 969–79.
42. Ligon BL. Penicillin: its discovery and early development. Semin Pediatr Infect Dis. 2004;15(1):52–7.
43. Shaik Mohamed Sayed UF, Moshawih S, Goh HP, Kifli N, Gupta G, Singh SK, et al. Natural products as novel anti-obesity agents: insights into mechanisms of action and potential for therapeutic management. Front Pharmacol. 2023 Jun 20;14:1182937.
44. Fu C, Jiang Y, Guo J, Su Z. Natural Products with Anti-obesity Effects and

Different Mechanisms of Action. J Agric Food Chem. 2016;64(51):9571–85.

45. Li S-Z, Zeng S-L, Liu E-H. Anti-obesity natural products and gut microbiota. Food Res Int. 2022 Jan;151:110819.
46. Mohamed GA, Ibrahim SRM, Elkhayat ES, El Dine RS. Natural anti-obesity agents. Bull Fac Pharmacy, Cairo Univ. 2014 Dec;52(2):269–84.
47. Wang S, Moustaid-Moussa N, Chen L, Mo H, Shastri A, Su R, et al. Novel insights of dietary polyphenols and obesity. J Nutr Biochem. 2014 Jan;25(1):1–18.
48. Haaz S, Fontaine KR, Cutter G, Limdi N, Perumean-Chaney S, Allison DB. Citrus aurantium and synephrine alkaloids in the treatment of overweight and obesity: an update. Obes Rev. 2006 Feb;7(1):79–88.
49. Yao N, Yan S, Guo Y, Wang H, Li X, Wang L, et al. The association between carotenoids and subjects with overweight or obesity: a systematic review and meta-analysis. Food Funct. 2021 Jun 8;12(11):4768–82.
50. Freitas S, Silva NG, Sousa ML, Ribeiro T, Rosa F, Leão PN, et al. Chlorophyll Derivatives from Marine Cyanobacteria with Lipid-Reducing Activities. Mar Drugs. 2019 Apr 17;17(4):229.
51. Carrasco del Amor A, Freitas S, Urbatzka R, Fresnedo O, Cristobal S. Application of Bioactive Thermal Proteome Profiling to Decipher the Mechanism of Action of the Lipid Lowering 132-Hydroxy-pheophytin Isolated from a Marine Cyanobacteria. Mar Drugs. 2019;17(6):371.
52. Deepika C, Wolf J, Roles J, Ross I, Hankamer B. Sustainable Production of Pigments from Cyanobacteria. In: Advances in Biochemical Engineering/Biotechnology. Adv Biochem Eng Biotechnol; 2022. p. 171–251.
53. Zhang C-C, Zhou C-Z, Burnap RL, Peng L. Carbon/Nitrogen Metabolic Balance: Lessons from Cyanobacteria. Trends Plant Sci. 2018 Dec;23(12):1116–30.
54. Häusler S, Weber M, de Beer D, Ionescu D. Spatial distribution of diatom and cyanobacterial mats in the Dead Sea is determined by response to rapid salinity fluctuations. Extremophiles. 2014 Nov 20;18(6):1085–94.
55. Rai AN. Cyanobacteria in Symbiosis. In: CRC Handbook of Symbiotic Cyanobacteria. CRC Press; 2018. p. 1–7.
56. Kumar K, Mella-Herrera RA, Golden JW. Cyanobacterial heterocysts. Cold Spring Harb Perspect Biol. 2010 Apr;2(4):a000315.
57. Garg R, Maldener I. The Formation of Spore-Like Akinetes: A Survival Strategy of Filamentous Cyanobacteria. Microb Physiol. 2021;31(3):296–305.
58. Risser DD. Hormogonium Development and Motility in Filamentous Cyanobacteria. Alexandre G, editor. Appl Environ Microbiol. 2023 Jun 28;89(6).

59. Strunecký O, Ivanova AP, Mareš J. An updated classification of cyanobacterial orders and families based on phylogenomic and polyphasic analysis. J Phycol. 2023 Feb 13;59(1):12–51.
60. Huisman J, Codd GA, Paerl HW, Ibelings BW, Verspagen JMH, Visser PM. Cyanobacterial blooms. Nat Rev Microbiol. 2018 Aug 26;16(8):471–83.
61. van Apeldoorn ME, van Egmond HP, Speijers GJA, Bakker GJI. Toxins of cyanobacteria. Mol Nutr Food Res. 2007 Jan;51(1):7–60.
62. Welker M, Dittmann E, von Döhren H. Cyanobacteria as a Source of Natural Products. In: Methods in Enzymology. Methods Enzymol; 2012. p. 23–46.
63. Borowitzka MA. Microalgae in Medicine and Human Health. In: Microalgae in Health and Disease Prevention. Elsevier; 2018. p. 195–210.
64. Nowicka-Krawczyk P, Mühlsteinová R, Hauer T. Detailed characterization of the Arthrospira type species separating commercially grown taxa into the new genus Limnospira (Cyanobacteria). Sci Rep. 2019 Jan 24;9(1):694.
65. Gutiérrez-Salmeán G, Fabila-Castillo L, Chamorro-Cevallos G. NUTRITIONAL AND TOXICOLOGICAL ASPECTS OF SPIRULINA (ARTHROSPIRA). Nutr Hosp. 2015;32(1):34–40.
66. Montalvo GEB, Vandenberghe LP de S, Soccol VT, Carvalho JC de, Soccol CR. The Antihypertensive, Antimicrobial and Anticancer Peptides from Arthrospira with Therapeutic Potential: A Mini Review. Curr Mol Med. 2020;20(8):593–606.
67. Ahmad AMR, Intikhab A, Zafar S, Farooq U, Shah HBU, Akram S, et al. Spirulina, an FDA-Approved Functional Food: Worth the Hype? Cell Mol Biol (Noisy-le-grand). 2023;69(1):137–44.
68. French Agency for Food E and OH& S. ANSES Opinion on the risks associated with the consumption of food supplements containing spirulina. 2017.
69. DiNicolantonio JJ, Bhat AG, OKeefe J. Effects of spirulina on weight loss and blood lipids: a review. Open Hear. 2020 Mar 8;7(1):e001003.
70. Rodríguez F, Garrido JL, Sobrino C, Johnsen G, Riobó P, Franco J, et al. Divinyl chlorophyll a in the marine eukaryotic protist Alexandrium ostenfeldii (Dinophyceae). Environ Microbiol. 2016 Feb 1;18(2):627–43.
71. Yilmaz C, Gökmen V. Chlorophyll. In: Encyclopedia of Food and Health. Elsevier; 2016. p. 37–41.
72. Tomitani A, Okada K, Miyashita H, Matthijs HCP, Ohno T, Tanaka A. Chlorophyll b and phycobilins in the common ancestor of cyanobacteria and chloroplasts. Nature. 1999 Jul 8;400(6740):159–62.
73. Solymosi K, Mysliwa-Kurdziel B. Chlorophylls and their Derivatives Used in Food Industry and Medicine. Mini Rev Med Chem. 2017;17(13):1194–222.

74. Kang Y-R, Park J, Jung SK, Chang YH. Synthesis, characterization, and functional properties of chlorophylls, pheophytins, and Zn-pheophytins. Food Chem. 2018 Apr 15;245:943–50.
75. Pucci C, Martinelli C, Degl'Innocenti A, Desii A, De Pasquale D, Ciofani G. Light-Activated Biomedical Applications of Chlorophyll Derivatives. Macromol Biosci. 2021;21(9):e2100181.
76. Zhang X-J, Liu M-H, Luo Y-S, Han G-Y, Ma Z-Q, Huang F, et al. Novel dual-mode antitumor chlorin-based derivatives as potent photosensitizers and histone deacetylase inhibitors for photodynamic therapy and chemotherapy. Eur J Med Chem. 2021 May 5;217:113363.
77. Liu Y, Lu Y, Chang Y, Chyuan J, Lee T, Hou W. Anti-adipogenic activities of pheophorbide a and pyropheophorbide a isolated from wild bitter gourd (Momordica charantia L. var. abbreviata Seringe) in vitro. J Sci Food Agric. 2022 Nov 17;102(14):6771–9.
78. Zang L, Maddison LA, Chen W. Zebrafish as a Model for Obesity and Diabetes. Front Cell Dev Biol. 2018 Aug 20;6(AUG):91.
79. MacRae CA, Peterson RT. Zebrafish as tools for drug discovery. Nat Rev Drug Discov. 2015 Oct;14(10):721–31.
80. Otis JP, Farber SA. High-fat Feeding Paradigm for Larval Zebrafish: Feeding, Live Imaging, and Quantification of Food Intake. J Vis Exp. 2016 Oct 27;2016(116).
81. Shimada Y, Hirano M, Nishimura Y, Tanaka T. A High-Throughput Fluorescence-Based Assay System for Appetite-Regulating Gene and Drug Screening. Gong Z, editor. PLoS One. 2012 Dec 26;7(12):e52549.
82. Wang F, Allen D, Tian S, Oler E, Gautam V, Greiner R, et al. CFM-ID 4.0 – a web server for accurate MS-based metabolite identification. Nucleic Acids Res. 2022 Jul 5;50(W1):W165–74.
83. Plotly. Plotly · Make charts and dashboards online. Plot.Ly. 2016.
84. da Silva RR, Wang M, Nothias L-F, van der Hooft JJJ, Caraballo-Rodríguez AM, Fox E, et al. Propagating annotations of molecular networks using in silico fragmentation. Schlessinger A, editor. PLOS Comput Biol. 2018;14(4):e1006089.
85. Mohimani H, Gurevich A, Mikheenko A, Garg N, Nothias L-F, Ninomiya A, et al. Dereplication of peptidic natural products through database search of mass spectra. Nat Chem Biol. 2017;13(1):30–7.
86. Wandy J, Zhu Y, van der Hooft JJJ, Daly R, Barrett MP, Rogers S. Ms2lda.org: web-based topic modelling for substructure discovery in mass spectrometry. Stegle O, editor. Bioinformatics. 2018;34(2):317–8.

87. Ernst M, Kang K Bin, Caraballo-Rodríguez AM, Nothias L-F, Wandy J, Chen C, et al. MolNetEnhancer: Enhanced Molecular Networks by Integrating Metabolome Mining and Annotation Tools. Metabolites. 2019;9(7):144.
88. Wang M, Carver JJ, Phelan V V., Sanchez LM, Garg N, Peng Y, et al. Sharing and community curation of mass spectrometry data with Global Natural Products Social Molecular Networking. Nat Biotechnol. 2016 Aug 9;34(8):828–37.
89. Shannon P, Markiel A, Ozier O, Baliga NS, Wang JT, Ramage D, et al. Cytoscape: A Software Environment for Integrated Models of Biomolecular Interaction Networks. Genome Res. 2003;13(11):2498–504.
90. Pumilia G, Cichon MJ, Cooperstone JL, Giuffrida D, Dugo G, Schwartz SJ. Changes in chlorophylls, chlorophyll degradation products and lutein in pistachio kernels (Pistacia vera L.) during roasting. Food Res Int. 2014 Nov 1;65(PB):193–8.
91. Pubchem. PubChem [Internet]. 2023. Available from: https://pubchem.ncbi.nlm.nih.gov/
92. Pagels F, Pereira RN, Vicente AA, Guedes AC. Extraction of pigments from microalgae and cyanobacteria-a review on current methodologies. Appl Sci. 2021 Jun 3;11(11):5187.
93. Hosikian A, Lim S, Halim R, Danquah MK. Chlorophyll Extraction from Microalgae: A Review on the Process Engineering Aspects. Int J Chem Eng. 2010;2010:1–11.
94. Society AC. Dichloromethane - American Chemical Society. 2019.
95. Choi WY, Lee HY. Enhancement of chlorophyll a production from marine Spirulina maxima by an optimized ultrasonic extraction process. Appl Sci. 2017 Dec 25;8(1).
96. Müller AH, Gough SP, Bollivar DW, Meldal M, Willows RD, Hansson M. Methods for the preparation of chlorophyllide a: An intermediate of the chlorophyll biosynthetic pathway. Anal Biochem. 2011 Dec 15;419(2):271–6.
97. Chen K, Ríos JJ, Pérez-Gálvez A, Roca M. Development of an accurate and high-throughput methodology for structural comprehension of chlorophylls derivatives. (I) Phytylated derivatives. J Chromatogr A. 2015 Aug 7;1406:99–108.
98. Chen K, Ríos JJ, Roca M, Pérez-Gálvez A. Development of an accurate and high-throughput methodology for structural comprehension of chlorophylls derivatives. (II) Dephytylated derivatives. J Chromatogr A. 2015 Sep 18;1412:90–9.
99. Regueiras A, Huguet Á, Conde T, Couto D, Domingues P, Domingues MR, et al.

Potential Anti-Obesity, Anti-Steatosis, and Anti-Inflammatory Properties of Extracts from the Microalgae Chlorella vulgaris and Chlorococcum amblystomatis under Different Growth Conditions. Mar Drugs. 2021 Dec 22;20(1):9.

100. Costa M, Rosa F, Ribeiro T, Hernandez-Bautista R, Bonaldo M, Gonçalves Silva N, et al. Identification of Cyanobacterial Strains with Potential for the Treatment of Obesity-Related Co-Morbidities by Bioactivity, Toxicity Evaluation and Metabolite Profiling. Mar Drugs. 2019 May 10;17(5):280.
101. Simon G, Bérubé C, Voyer N, Grenier D. Anti-biofilm and anti-adherence properties of novel cyclic dipeptides against oral pathogens. Bioorg Med Chem. 2019 Jun 15;27(12):2323–31.
102. KGK D, Kumari S, G S, Malla RR. Marine natural compound cyclo(L-leucyl-L-prolyl) peptide inhibits migration of triple negative breast cancer cells by disrupting interaction of CD151 and EGFR signaling. Chem Biol Interact. 2020 Jan 5;315:108872.
103. Dahlhoff C, Worsch S, Sailer M, Hummel BA, Fiamoncini J, Uebel K, et al. Methyl-donor supplementation in obese mice prevents the progression of NAFLD, activates AMPK and decreases acyl-carnitine levels. Mol Metab. 2014 Aug 1;3(5):565–80.
104. Kinnamon SC. Umami taste transduction mechanisms. Am J Clin Nutr. 2009 Sep 1;90(3).
105. Niu K, Bai P, Zhang J, Feng X, Qiu F. Cytidine Alleviates Dyslipidemia and Modulates the Gut Microbiota Composition in ob/ob Mice. Nutrients. 2023 Feb 24;15(5):1147.
106. Pardo F, Villalobos-Labra R, Chiarello DI, Salsoso R, Toledo F, Gutierrez J, et al. Molecular implications of adenosine in obesity. Mol Aspects Med. 2017 Jun 1;55:90–101.
107. Levine AS, Morley JE. Effect of intraventricular adenosine on food intake in rats. Pharmacol Biochem Behav. 1983 Jul;19(1):23–6.
108. Beelman RB, Kalaras MD, Phillips AT, Richie JP. Is ergothioneine a 'longevity vitamin' limited in the American diet? J Nutr Sci. 2020 Nov 11;9:e52.
109. Fu T-T, Shen L. Ergothioneine as a Natural Antioxidant Against Oxidative Stress-Related Diseases. Front Pharmacol. 2022 Mar 18;13.
110. Lam-Sidun D, Peters KM, Borradaile NM. Mushroom-Derived Medicine? Preclinical Studies Suggest Potential Benefits of Ergothioneine for Cardiometabolic Health. Int J Mol Sci. 2021 Mar 23;22(6):3246.
111. Calvo MS, Mehrotra A, Beelman RB, Nadkarni G, Wang L, Cai W, et al. A

Retrospective Study in Adults with Metabolic Syndrome: Diabetic Risk Factor Response to Daily Consumption of Agaricus bisporus (White Button Mushrooms). Plant Foods Hum Nutr. 2016 Sep 1;71(3):245–51.

112. CARNEY BI, JONES KL, HOROWITZ M, SUN WM, HEBBARD G, EDELBROEK MAL. Stereospecific effects of tryptophan on gastric emptying and hunger in humans. J Gastroenterol Hepatol. 1994 Dec 10;9(6):557–63.

113. Goodarzi P, Habibi M, Roberts K, Sutton J, Shili CN, Lin D, et al. Dietary Tryptophan Supplementation Alters Fat and Glucose Metabolism in a Low-Birthweight Piglet Model. 2021;1–22.

8. Appendix

Table S1 – Data used for the relative quantification of chlorophyll a and its derivatives in all the performed extractions. Retention time (Rt).

Compound	Sample	Calculated *m/z* $[M+H]^+$	Experimental *m/z* $[M+H]^+$	Ppm mass error	Peak Area	Rt (min)
Chlorophyll a	M1	893.543153	-	-	0.00E+00	-
	E1	893.543153	-	-	0.00E+00	-
	A1	893.543153	-	-	0.00E+00	-
	D1	893.543153	-	-	0.00E+00	-
	M2	893.543153	-	-	0.00E+00	-
	E2	893.543153	-	-	0.00E+00	-
	A2	893.543153	893.5416	1.738024621	4.38E+07	13.18
	D2	893.543153	893.5416	1.738024621	5.01E+06	13.17
	M3	893.543153	-	-	0.00E+00	-
	E3	893.543153	-	-	0.00E+00	-
	A3	893.543153	-	-	0.00E+00	-
	D3	893.543153	893.5408	2.633336725	1.64E+08	13.16
	M4	893.543153	-	-	0.00E+00	-
	E4	893.543153	-	-	0.00E+00	-
	A4	893.543153	-	-	0.00E+00	-
	D4	893.543153	893.5411	2.297594686	1.39E+08	13.15
	E5a	893.543153	-	-	0.00E+00	-
	E5b	893.543153	-	-	0.00E+00	-
	E5c	893.543153	-	-	0.00E+00	-
	E6a	893.543153	-	-	0.00E+00	-
	E6b	893.543153	-	-	0.00E+00	-
	E6c	893.543153	-	-	0.00E+00	-
	E7a	893.543153	-	-	0.00E+00	-
	E7b	893.543153	-	-	0.00E+00	-
	E7c	893.543153	-	-	0.00E+00	-
	E8a	893.543153	-	-	0.00E+00	-
	E8b	893.543153	-	-	0.00E+00	-
	E8c	893.543153	-	-	0.00E+00	-
Chlorophyll a'	M1	893.543153	-	-	0.00E+00	-
	E1	893.543153	-	-	0.00E+00	-
	A1	893.543153	-	-	0.00E+00	-
	D1	893.543153	893.5418	1.514196595	7.37E+07	13.39
	M2	893.543153	-	-	0.00E+00	-
	E2	893.543153	-	-	0.00E+00	-
	A2	893.543153	-	-	0.00E+00	-
	D2	893.543153	-	-	0.00E+00	-
	M3	893.543153	-	-	0.00E+00	-
	E3	893.543153	-	-	0.00E+00	-
	A3	893.543153	-	-	0.00E+00	-

	D3	893.543153	893.5407	2.745250738	1.47E+08	13.4
	M4	893.543153	-	-	0.00E+00	-
	E4	893.543153	-	-	0.00E+00	-
	A4	893.543153	-	-	0.00E+00	-
	D4	893.543153	893.5414	1.961852647	1.21E+08	13.38
	E5a	893.543153	-	-	0.00E+00	-
	E5b	893.543153	-	-	0.00E+00	-
	E5c	893.543153	-	-	0.00E+00	-
	E6a	893.543153	-	-	0.00E+00	-
	E6b	893.543153	-	-	0.00E+00	-
	E6c	893.543153	-	-	0.00E+00	-
	E7a	893.543153	-	-	0.00E+00	-
	E7b	893.543153	-	-	0.00E+00	-
	E7c	893.543153	-	-	0.00E+00	-
	E8a	893.543153	-	-	0.00E+00	-
	E8b	893.543153	-	-	0.00E+00	-
	E8c	893.543153	-	-	0.00E+00	-
Chlorophyllide a	M1	615.2458019	-	-	0.00E+00	-
	E1	615.2458019	-	-	0.00E+00	-
	A1	615.2458019	-	-	0.00E+00	-
	D1	615.2458019	-	-	0.00E+00	-
	M2	615.2458019	-	-	0.00E+00	-
	E2	615.2458019	-	-	0.00E+00	-
	A2	615.2458019	-	-	0.00E+00	-
	D2	615.2458019	-	-	0.00E+00	-
	M3	615.2458019	-	-	0.00E+00	-
	E3	615.2458019	-	-	0.00E+00	-
	A3	615.2458019	-	-	0.00E+00	-
	D3	615.2458019	-	-	0.00E+00	-
	M4	615.2458019	-	-	0.00E+00	-
	E4	615.2458019	-	-	0.00E+00	-
	A4	615.2458019	-	-	0.00E+00	-
	D4	615.2458019	-	-	0.00E+00	-
	E5a	615.2458019	-	-	0.00E+00	-
	E5b	615.2458019	-	-	0.00E+00	-
	E5c	615.2458019	-	-	0.00E+00	-
	E6a	615.2458019	-	-	0.00E+00	-
	E6b	615.2458019	-	-	0.00E+00	-
	E6c	615.2458019	-	-	0.00E+00	-
	E7a	615.2458019	-	-	0.00E+00	-
	E7b	615.2458019	-	-	0.00E+00	-
	E7c	615.2458019	-	-	0.00E+00	-
	E8a	615.2458019	-	-	0.00E+00	-
	E8b	615.2458019	-	-	0.00E+00	-
	E8c	615.2458019	-	-	0.00E+00	-

Pheophytin a	M1	871.573761	871.5724	1.561543108	2.89E+08	14.11
	E1	871.573761	871.5722	1.791013073	1.20E+09	14.07
	A1	871.573761	871.5724	1.561543108	1.57E+08	14.09
	D1	871.573761	871.5723	1.676278091	5.19E+08	14.08
	M2	871.573761	871.5729	0.987868197	1.95E+09	14.08
	E2	871.573761	871.5729	0.987868197	2.65E+06	14.13
	A2	871.573761	871.5721	1.905748055	1.95E+09	14.09
	D2	871.573761	871.5728	1.102603179	4.01E+07	14.09
	M3	871.573761	871.5723	1.676278091	5.16E+08	14.08
	E3	871.573761	871.5722	1.791013073	2.79E+09	14.08
	A3	871.573761	871.5727	1.217338162	8.94E+07	14.1
	D3	871.573761	871.5722	1.791013073	2.30E+09	14.07
	M4	871.573761	871.5725	1.446808126	1.14E+09	14.09
	E4	871.573761	871.572	2.020483037	1.85E+09	14.09
	A4	871.573761	871.5717	2.364687984	1.63E+09	14.09
	D4	871.573761	871.5717	2.364687984	1.75E+09	14.08
	E5a	871.573761	871.571	3.16783286	7.84E+08	14.02
	E5b	871.573761	871.5709	3.282567842	2.60E+09	14
	E5c	871.573761	871.5709	3.282567842	2.51E+09	14.01
	E6a	871.573761	871.5715	2.594157949	3.04E+08	14.01
	E6b	871.573761	871.5712	2.938362896	1.23E+09	14
	E6c	871.573761	871.572	2.020483037	1.91E+07	14.01
	E7a	871.573761	871.5712	2.938362896	1.61E+09	14.01
	E7b	871.573761	871.5714	2.708892931	1.63E+08	14.01
	E7c	871.573761	871.5715	2.594157949	6.26E+07	14
	E8a	871.573761	871.571	3.16783286	3.28E+09	14
	E8b	871.573761	871.5717	2.364687984	5.95E+07	14
	E8c	871.573761	871.5713	2.823627913	2.06E+08	14.01
Pheophytin a'	M1	871.573761	871.5728	1.102603179	8.49E+07	14.35
	E1	871.573761	871.5715	2.594157949	6.39E+08	14.35
	A1	871.573761	871.5724	1.561543108	6.19E+08	14.33
	D1	871.573761	871.5724	1.561543108	4.16E+08	14.33
	M2	871.573761	871.5717	2.364687984	1.20E+09	14.34
	E2	871.573761	-	-	0.00E+00	-
	A2	871.573761	871.5711	3.053097878	5.80E+08	14.39
	D2	871.573761	871.5729	0.987868197	1.95E+07	14.37
	M3	871.573761	871.5718	2.249953002	4.65E+08	14.35
	E3	871.573761	871.5718	2.249953002	8.96E+08	14.36
	A3	871.573761	871.5726	1.332073144	3.74E+07	14.37
	D3	871.573761	871.5717	2.364687984	5.43E+08	14.36
	M4	871.573761	871.5717	2.364687984	4.77E+08	14.36
	E4	871.573761	871.5715	2.594157949	1.61E+09	14.38
	A4	871.573761	871.5717	2.364687984	1.15E+09	14.34
	D4	871.573761	871.5715	2.594157949	6.54E+08	14.36
	E5a	871.573761	871.5712	2.938362896	3.15E+09	14.25

	E5b	871.573761	871.571	3.16783286	3.18E+08	14.23
	E5c	871.573761	871.571	3.16783286	9.09E+08	14.24
	E6a	871.573761	871.5712	2.938362896	3.52E+08	14.25
	E6b	871.573761	871.5721	1.905748055	8.08E+08	14.25
	E6c	871.573761	-	-	0.00E+00	-
	E7a	871.573761	871.5712	2.938362896	4.91E+08	14.24
	E7b	871.573761	871.5715	2.594157949	7.20E+07	14.25
	E7c	871.573761	871.5719	2.13521802	1.80E+07	14.25
	E8a	871.573761	871.5712	2.938362896	1.21E+09	14.25
	E8b	871.573761	871.5723	1.676278091	1.37E+07	14.24
	E8c	871.573761	871.5716	2.479422966	1.09E+08	14.24
13²-Hydroxy-pheophytin a	M1	887.5697	887.566	4.168686696	2.15E+09	13.7
	E1	887.5697	887.5663	3.830685072	1.76E+09	13.69
	A1	887.5697	887.5659	4.281353904	8.06E+08	13.7
	D1	887.5697	887.5663	3.830685072	1.14E+09	13.7
	M2	887.5697	887.5662	3.94335228	1.85E+09	13.7
	E2	887.5697	-	-	0.00E+00	-
	A2	887.5697	887.5665	3.605350656	1.05E+09	13.7
	D2	887.5697	887.5676	2.366011368	1.40E+07	13.71
	M3	887.5697	887.5665	3.605350656	1.91E+09	13.69
	E3	887.5697	887.5663	3.830685072	1.00E+09	13.7
	A3	887.5697	887.5667	3.38001624	2.44E+08	13.71
	D3	887.5697	887.5665	3.605350656	9.59E+08	13.71
	M4	887.5697	887.5663	3.830685072	1.94E+09	13.71
	E4	887.5697	887.5663	3.830685072	2.03E+09	13.71
	A4	887.5697	887.5662	3.94335228	1.17E+09	13.71
	D4	887.5697	887.5665	3.605350656	7.82E+08	13.7
	E5a	887.5697	887.566	4.168686696	1.18E+09	13.66
	E5b	887.5697	887.566	4.168686696	2.37E+09	13.65
	E5c	887.5697	887.566	4.168686696	1.69E+09	13.66
	E6a	887.5697	887.5663	3.830685072	2.31E+08	13.64
	E6b	887.5697	887.5663	3.830685072	1.81E+09	13.64
	E6c	887.5697	887.5667	3.38001624	1.19E+07	13.64
	E7a	887.5697	887.5663	3.830685072	2.39E+08	13.62
	E7b	887.5697	887.5664	3.718017864	7.04E+07	13.61
	E7c	887.5697	887.5665	3.605350656	8.00E+07	13.62
	E8a	887.5697	887.5662	3.94335228	6.40E+08	13.62
	E8b	887.5697	887.5666	3.492683448	5.77E+07	13.62
	E8c	887.5697	887.5663	3.830685072	1.27E+08	13.62
13²-Hydroxy-pheophytin a'	M1	887.5697	887.5662	3.94335228	7.66E+08	13.86
	E1	887.5697	887.5667	3.38001624	4.25E+08	13.86
	A1	887.5697	887.5664	3.718017864	1.39E+09	13.86
	D1	887.5697	887.5664	3.718017864	3.51E+08	13.85
	M2	887.5697	887.5673	2.704012992	1.94E+08	13.84
	E2	887.5697	-	-	0.00E+00	-

	A2	887.5697	887.5665	3.605350656	1.63E+09	13.88
	D2	887.5697	887.5678	2.140676952	4.52E+06	13.88
	M3	887.5697	887.5667	3.38001624	2.21E+07	13.86
	E3	887.5697	887.5668	3.267349032	6.08E+07	13.85
	A3	887.5697	887.5668	3.267349032	1.29E+06	13.85
	D3	887.5697	887.5664	3.718017864	3.50E+07	13.87
	M4	887.5697	887.5669	3.154681824	5.39E+08	13.87
	E4	887.5697	887.5667	3.38001624	4.45E+08	13.87
	A4	887.5697	887.5665	3.605350656	9.67E+08	13.87
	D4	887.5697	887.5668	3.267349032	2.41E+08	13.85
	E5a	887.5697	887.5662	3.94335228	1.37E+09	13.78
	E5b	887.5697	887.5662	3.94335228	6.11E+08	13.78
	E5c	887.5697	887.5662	3.94335228	1.05E+09	13.77
	E6a	887.5697	887.5667	3.38001624	2.26E+08	13.79
	E6b	887.5697	887.5666	3.492683448	7.98E+08	13.77
	E6c	887.5697	887.5667	3.38001624	1.54E+07	13.76
	E7a	887.5697	887.5663	3.830685072	1.33E+08	13.74
	E7b	887.5697	887.5664	3.718017864	3.65E+07	13.74
	E7c	887.5697	887.5663	3.830685072	8.59E+07	13.74
	E8a	887.5697	887.5663	3.830685072	2.28E+08	13.75
	E8b	887.5697	887.5665	3.605350656	6.46E+07	13.75
	E8c	887.5697	887.5666	3.492683448	1.79E+08	13.75
Pyropheophytin a	M1	813.5677	-	-	0.00E+00	-
	E1	813.5677	-	-	0.00E+00	-
	A1	813.5677	-	-	0.00E+00	-
	D1	813.5677	-	-	0.00E+00	-
	M2	813.5677	-	-	0.00E+00	-
	E2	813.5677	-	-	0.00E+00	-
	A2	813.5677	-	-	0.00E+00	-
	D2	813.5677	-	-	0.00E+00	-
	M3	813.5677	-	-	0.00E+00	-
	E3	813.5677	-	-	0.00E+00	-
	A3	813.5677	-	-	0.00E+00	-
	D3	813.5677	-	-	0.00E+00	-
	M4	813.5677	-	-	0.00E+00	-
	E4	813.5677	-	-	0.00E+00	-
	A4	813.5677	-	-	0.00E+00	-
	D4	813.5677	-	-	0.00E+00	-
	E5a	813.5677	813.5658	2.335392617	4.77E+07	14.88
	E5b	813.5677	813.5659	2.212477216	6.36E+07	14.88
	E5c	813.5677	813.5657	2.458308018	7.85E+07	14.88
	E6a	813.5677	813.566	2.089561815	3.17E+07	14.88
	E6b	813.5677	813.5656	2.581223419	2.03E+08	14.88
	E6c	813.5677	813.5661	1.966646414	3.18E+07	14.88

	E7a	813.5677	813.5663	1.720815613	1.96E+07	14.88
	E7b	813.5677	813.5671	0.737492405	1.35E+06	14.88
	E7c	813.5677	813.5671	0.737492405	9.26E+05	14.88
	E8a	813.5677	813.5656	2.581223419	1.41E+08	14.88
	E8b	813.5677	813.566	2.089561815	5.86E+07	14.88
	E8c	813.5677	813.5657	2.458308018	2.04E+08	14.88
Pyropheophytin a'	M1	813.5677	813.5664	1.597900212	2.08E+07	15.18
	E1	813.5677	813.5665	1.474984811	1.39E+07	15.18
	A1	813.5677	813.5663	1.720815613	2.72E+07	15.18
	D1	813.5677	813.5663	1.720815613	3.70E+07	15.18
	M2	813.5677	813.5667	1.229154009	9.38E+06	15.15
	E2	813.5677	-	-	0.00E+00	-
	A2	813.5677	813.5673	0.491661603	6.01E+07	15.19
	D2	813.5677	-	-	0.00E+00	-
	M3	813.5677	813.567	0.860407806	4.95E+06	15.18
	E3	813.5677	813.5666	1.35206941	2.36E+07	15.18
	A3	813.5677	813.5673	0.491661603	1.78E+06	15.18
	D3	813.5677	813.5662	1.843731013	7.03E+07	15.18
	M4	813.5677	813.5663	1.720815613	2.51E+07	15.18
	E4	813.5677	813.5667	1.229154009	1.87E+07	15.18
	A4	813.5677	813.5669	0.983323207	8.16E+06	15.18
	D4	813.5677	813.5663	1.720815613	7.70E+07	15.18
	E5a	813.5677	-	-	0.00E+00	-
	E5b	813.5677	-	-	0.00E+00	-
	E5c	813.5677	-	-	0.00E+00	-
	E6a	813.5677	-	-	0.00E+00	-
	E6b	813.5677	-	-	0.00E+00	-
	E6c	813.5677	-	-	0.00E+00	-
	E7a	813.5677	-	-	0.00E+00	-
	E7b	813.5677	-	-	0.00E+00	-
	E7c	813.5677	-	-	0.00E+00	-
	E8a	813.5677	-	-	0.00E+00	-
	E8b	813.5677	-	-	0.00E+00	-
	E8c	813.5677	-	-	0.00E+00	-
Pheophorbide a	M1	593.276411	-	-	0.00E+00	-
	E1	593.276411	-	-	0.00E+00	-
	A1	593.276411	-	-	0.00E+00	-
	D1	593.276411	-	-	0.00E+00	-
	M2	593.276411	-	-	0.00E+00	-
	E2	593.276411	-	-	0.00E+00	-
	A2	593.276411	-	-	0.00E+00	-
	D2	593.276411	-	-	0.00E+00	-
	M3	593.276411	-	-	0.00E+00	-
	E3	593.276411	-	-	0.00E+00	-
	A3	593.276411	-	-	0.00E+00	-

	D3	593.276411	-	-	0.00E+00	-
	M4	593.276411	-	-	0.00E+00	-
	E4	593.276411	-	-	0.00E+00	-
	A4	593.276411	-	-	0.00E+00	-
	D4	593.276411	-	-	0.00E+00	-
	E5a	593.276411	593.2755	1.535540573	1.85E+08	11.23
	E5b	593.276411	593.2753	1.872651566	1.53E+08	11.23
	E5c	593.276411	-	-	0.00E+00	-
	E6a	593.276411	593.2754	1.704096069	1.27E+08	11.19
	E6b	593.276411	593.2751	2.209762559	1.31E+08	11.2
	E6c	593.276411	-	-	0.00E+00	-
	E7a	593.276411	593.2747	2.883984545	2.80E+09	11.19
	E7b	593.276411	593.2753	1.872651566	1.76E+08	11.19
	E7c	593.276411	593.2748	2.715429048	2.05E+08	11.18
	E8a	593.276411	593.2748	2.715429048	1.50E+09	11.18
	E8b	593.276411	593.2753	1.872651566	1.12E+08	11.21
	E8c	593.276411	593.2753	1.872651566	1.92E+08	11.21
Pheophorbide a'	M1	593.276411	-	-	0.00E+00	-
	E1	593.276411	-	-	0.00E+00	-
	A1	593.276411	-	-	0.00E+00	-
	D1	593.276411	-	-	0.00E+00	-
	M2	593.276411	-	-	0.00E+00	-
	E2	593.276411	-	-	0.00E+00	-
	A2	593.276411	593.2754	1.704096069	8.44E+08	11.31
	D2	593.276411	-	-	0.00E+00	-
	M3	593.276411	-	-	0.00E+00	-
	E3	593.276411	593.2753	1.872651566	1.71E+08	11.34
	A3	593.276411	-	-	0.00E+00	-
	D3	593.276411	-	-	0.00E+00	-
	M4	593.276411	-	-	0.00E+00	-
	E4	593.276411	-	-	0.00E+00	-
	A4	593.276411	-	-	0.00E+00	-
	D4	593.276411	-	-	0.00E+00	-
	E5a	593.276411	-	-	0.00E+00	-
	E5b	593.276411	-	-	0.00E+00	-
	E5c	593.276411	-	-	0.00E+00	-
	E6a	593.276411	-	-	0.00E+00	-
	E6b	593.276411	-	-	0.00E+00	-
	E6c	593.276411	-	-	0.00E+00	-
	E7a	593.276411	593.2745	3.221095538	2.25E+08	11.29
	E7b	593.276411	593.2754	1.704096069	6.76E+06	11.29
	E7c	593.276411	593.2747	2.883984545	1.27E+08	11.3
	E8a	593.276411	593.2749	2.546873552	4.90E+07	11.28
	E8b	593.276411	593.2755	1.535540573	3.13E+06	11.3
	E8c	593.276411	-	-	0.00E+00	-

Pyropheophorbide a	M1	535.270931	-	-	0.00E+00	-
	E1	535.270931	-	-	0.00E+00	-
	A1	535.270931	-	-	0.00E+00	-
	D1	535.270931	-	-	0.00E+00	-
	M2	535.270931	-	-	0.00E+00	-
	E2	535.270931	-	-	0.00E+00	-
	A2	535.270931	-	-	0.00E+00	-
	D2	535.270931	-	-	0.00E+00	-
	M3	535.270931	-	-	0.00E+00	-
	E3	535.270931	-	-	0.00E+00	-
	A3	535.270931	-	-	0.00E+00	-
	D3	535.270931	-	-	0.00E+00	-
	M4	535.270931	-	-	0.00E+00	-
	E4	535.270931	-	-	0.00E+00	-
	A4	535.270931	-	-	0.00E+00	-
	D4	535.270931	-	-	0.00E+00	-
	E5a	535.270931	535.2702	1.36566355	2.76E+07	11.71
	E5b	535.270931	535.27	1.739306109	4.01E+07	11.72
	E5c	535.270931	535.2701	1.55248483	3.67E+07	11.71
	E6a	535.270931	535.27	1.739306109	4.92E+06	11.69
	E6b	535.270931	535.2695	2.673412504	4.75E+07	11.7
	E6c	535.270931	535.2693	3.047055062	5.03E+07	11.7
	E7a	535.270931	535.2692	3.233876342	1.42E+08	11.7
	E7b	535.270931	535.2698	2.112948667	1.14E+08	11.7
	E7c	535.270931	535.2695	2.673412504	6.32E+07	11.69
	E8a	535.270931	535.2692	3.233876342	1.62E+08	11.7
	E8b	535.270931	5.35E+02	3.233876342	3.91E+08	11.7
	E8c	535.270931	535.2691	3.420697621	2.46E+08	11.69

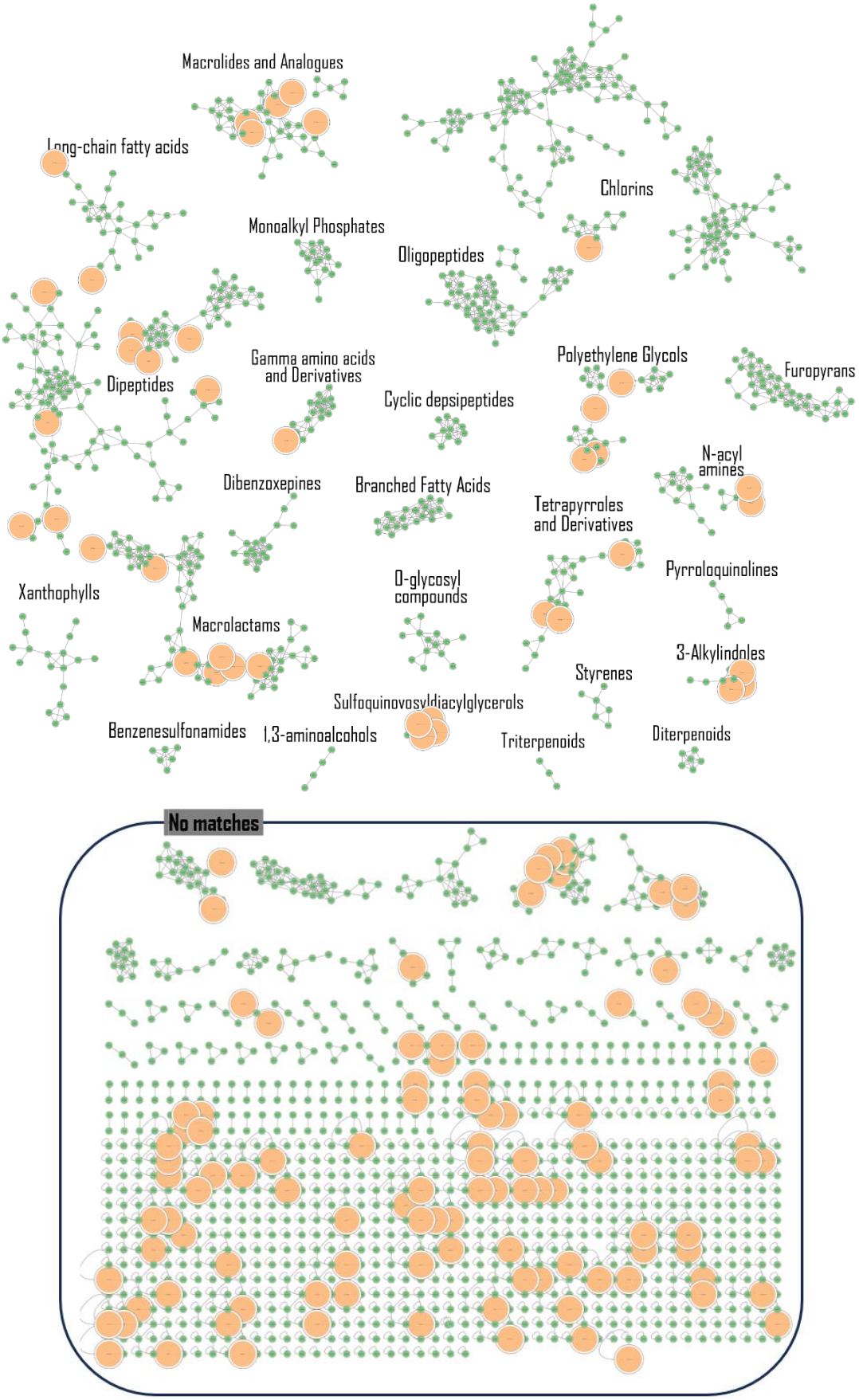

Figure S1 – **Metabolite Profiling of Prospecting Extractions with Appetite-reducing Activity.** Unique nodes found exclusively in appetite-reducing bioactive extract A3 are highlighted in larger size and orange-coloured.

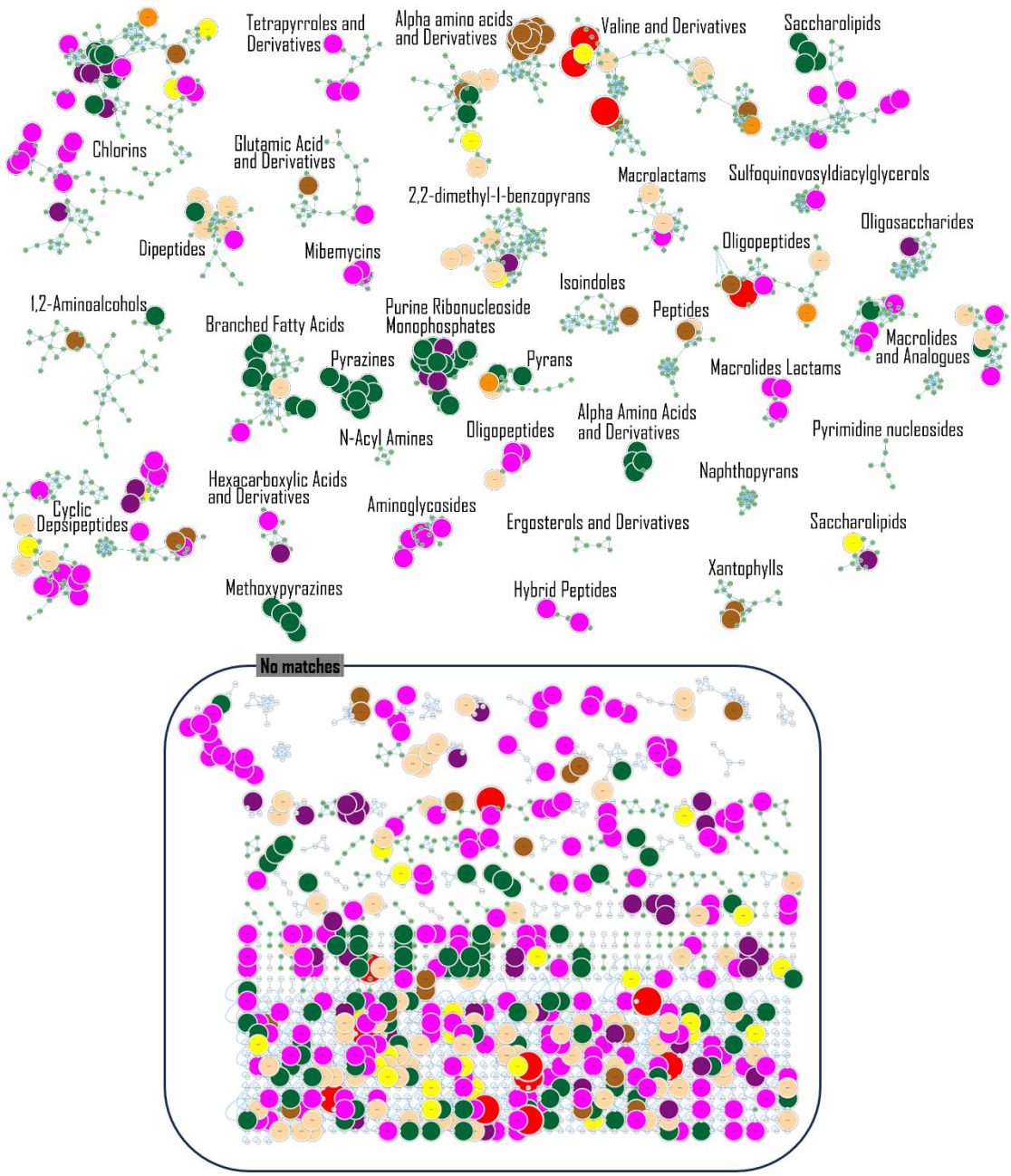

Figure S2 – **Metabolite Profiling of Targeted Extractions with Lipid-reducing Activity.** Unique nodes found exclusively in lipid-reducing bioactive extracts E5a (yellow), E5b (orange), E6a (beige), E6b (brown), E6c (dark green), E7c (pink), and E8c (purple) are highlighted in larger sizes. Nodes found in all these extracts have a higher size and red colour.

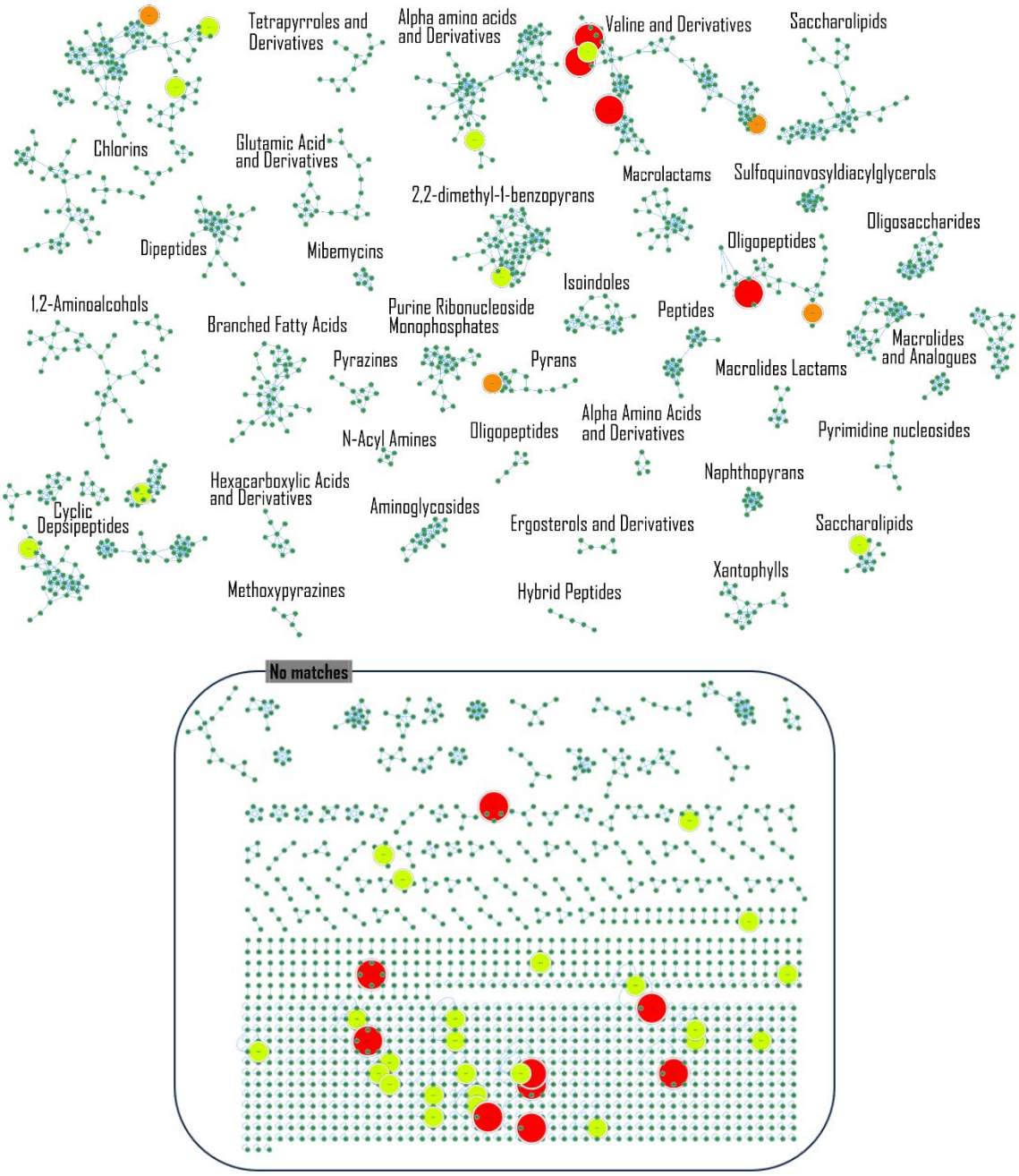

Figure S3 – **Metabolite Profiling of Targeted Extractions with Appetite-reducing Activity.** Unique nodes found exclusively in appetite-reducing bioactive extracts E5a (yellow) and E5b (orange) are highlighted in larger sizes. Nodes found in both extracts have a higher size and red colour.